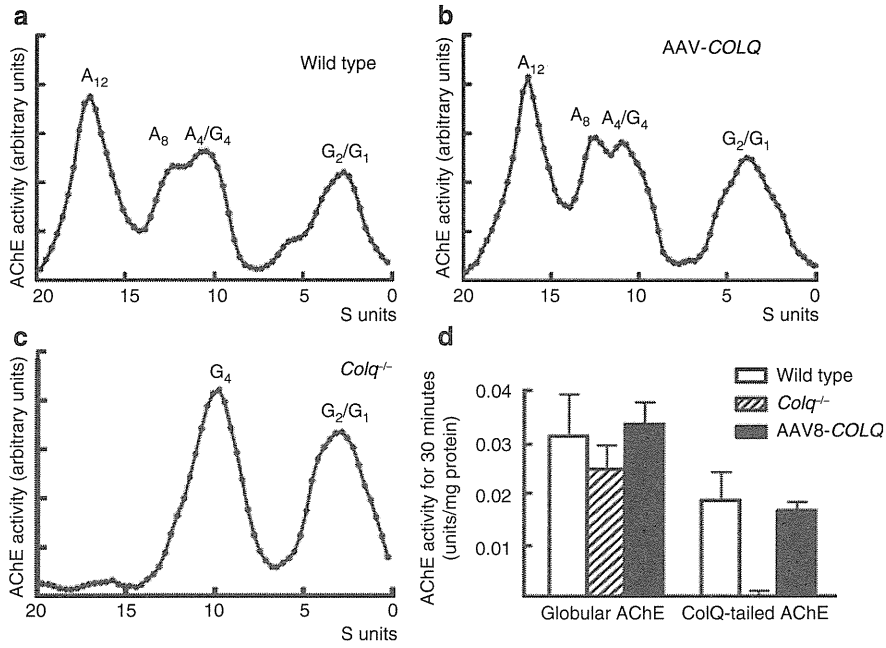

Figure 5 Quantification and biochemical analysis of acetylcholinesterase (AChE) recovery in muscles. Intravenous injection of 2×10^{12} vg of AAV8-*COLQ* into (**b**) *Colq*$^{-/-}$ mice gives rise to a sedimentation profile that is identical to that of (**a**) wild type, whereas (**c**) *Colq*$^{-/-}$ mice carry no collagen Q (ColQ)-tailed AChE. A_4, A_8, and A_{12} species carry 4, 8, and 12 AChE catalytic subunits attached to a triple helical ColQ. G_1, G_2, and G_4 species carry 1, 2, and 4 AChE catalytic subunits but without ColQ. A representative profile of three experiments is indicated. (**d**) Quantification of globular and ColQ-tailed AChE species (mean and SD, $n = 4$). The activity of ColQ-tailed AChE in the skeletal muscle of AAV8-*COLQ* mice is restored to 89 ± 10% of that of wild type. AAV8, adeno-associated virus serotype 8.

NMJs in noninjected muscles (data not shown). These results, however, could not exclude the possibility that AAV8-*COLQ* had been delivered to noninjected muscles in the form of a virus.

Local intramuscular injection of AAV1-*COLQ-IRES-EGFP* expresses ColQ-tailed AChE at NMJs of noninjected limbs

To reduce systemic delivery of AAV8 and to identify infected cells, we packed *COLQ* cDNA into the AAV serotype 1 (AAV1) that is known to transduce the injected muscle fibers locally.[19] In addition, we fused *COLQ* and internal ribosome entry site (*IRES*)-*EGFP* to express green fluorescent protein (GFP) in transduced cells synthesizing ColQ. We injected 2×10^{11} vg of AAV1-*COLQ-IRES-EGFP* into the left anterior tibial muscle of *Colq*$^{-/-}$ mice, while blocking the blood flow with a tourniquet for 20 minutes to restrict the distribution of the virus. The transduction efficiencies of AAV1-*COLQ-IRES-EGFP* were as follows: left anterior tibial muscle, 1.70 ± 0.29 viral copies per nucleus; right gastrocnemius muscle, 0.00100 ± 0.00079 copies; and bilateral brachial muscles, 0.00126 ± 0.00058 copies (mean ± SD, $n = 3$). Although only a fraction of the injected AAV1-*COLQ-IRES-EGFP* moved to noninjected limbs, we observed colocalization of ColQ and AChE at all the examined NMJs of right gastrocnemius, right tibialis anterior, both triceps, and both biceps in four examined mice (**Figure 6a**). We analyzed a total of 200–400 NMJs per muscle. In contrast, expression of intracellular enhanced GFP (EGFP) was not observed in noninjected limb muscles. We also quantified ColQ-tailed AChE in the noninjected bilateral forelimbs and right hindlimb, and found that the amounts were 21.5 ± 10.2% and 28.4 ± 10.0% (mean ± SD, $n = 4$), respectively, of those of wild type (**Figure 6b**).

ColQ-tailed AChE protein reaches and binds to remote NMJs

The presence of ColQ in noninjected muscles strongly suggests that the ColQ-tailed AChE is assembled intracellularly in one muscle and has moved to noninjected muscles, where it is anchored to the NMJs. To directly test this possibility, the gluteus maximus muscles of 5-week-old *Colq*$^{-/-}$ mice ($n = 4$) were injected daily with 2 μg of recombinant human ColQ-tailed AChE for 7 days. Histological analysis revealed the presence of ColQ and AChE in all of the examined NMJs from triceps muscles (**Figure 7a**). Quantitative analysis of ColQ signal intensities at the NMJs of noninjected triceps demonstrated that the ColQ-positive areas normalized for the AChR-positive area per NMJ became indistinguishable from that of wild type (**Figure 7b**). Furthermore, the ColQ signal intensity normalized for the AChR area per NMJs reached ~41.6% of that of wild type (**Figure 7c**). The *Colq*$^{-/-}$ mice could not hang on the wire at all, but the protein-injected mice acquired the ability to hang on the wire for two or more minutes from the fourth day of injection.

DISCUSSION

Effective and persistent gene therapy of ColQ with a single intravenous injection of AAV8-*COLQ*

We present an efficient and persistent recovery of AChE at the NMJ after a single intravenous administration of AAV8-*COLQ* in a *Colq*$^{-/-}$ mouse model of congenital myasthenic syndrome

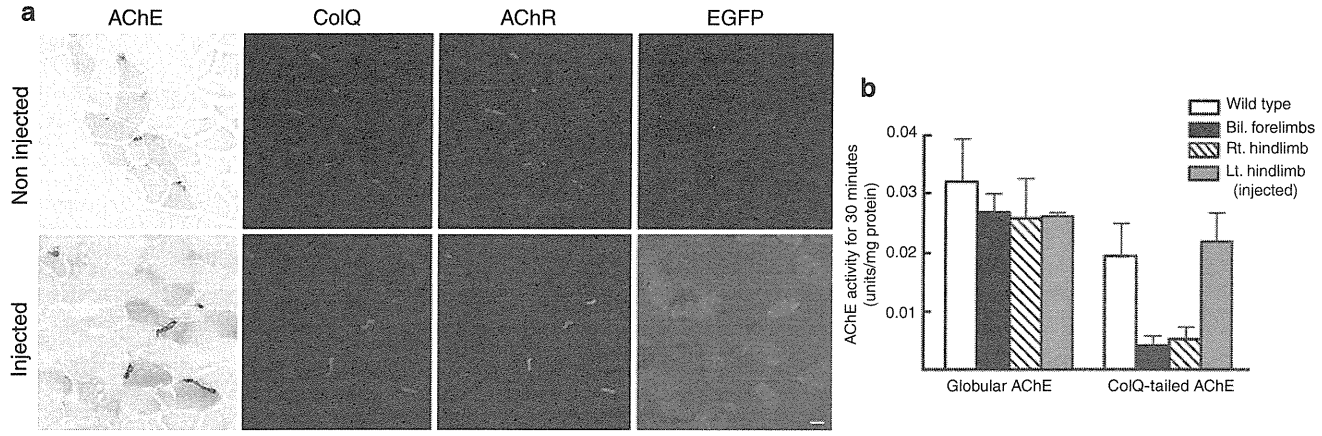

Figure 6 Intramuscular injection of 2×10^{11} vg of AAV1-*COLQ-IRES-EGFP* into the left anterior tibial muscle of *Colq*$^{-/-}$ mice. (**a**) Acetylcholinesterase (AChE) activity and collagen Q (ColQ) are colocalized to the acetylcholine receptors (AChR) in the injected muscle, as well as in the noninjected triceps muscle, although the signal intensities are not as high as those of the injected muscle. In contrast to ColQ, an intracellular molecule, enhanced green fluorescent protein (EGFP), is expressed only in the injected muscle, but not in the noninjected muscle. Bar = 10 µm. (**b**) Quantification of globular and ColQ-tailed AChE species of skeletal muscles (mean and SD, $n = 4$). In the injected left hindlimb, the activity of ColQ-tailed AChE is similar to that of wild type. In the noninjected both forelimbs and right hindlimb, the activities are 21.5 and 28.4% of wild type, respectively. AAV1, adeno-associated virus serotype 1.

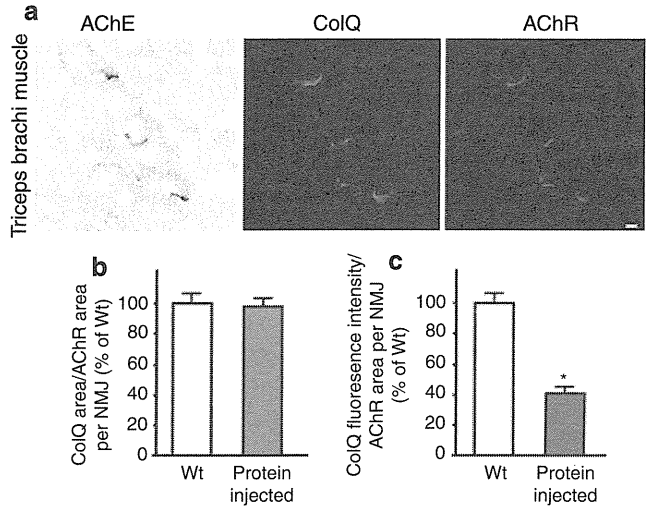

Figure 7 Injection of purified recombinant human collagen Q (ColQ)-tailed acetylcholinesterase (AChE). (**a**) Daily injection of 0.2 µg human recombinant ColQ-tailed AChE into the gluteus maximus muscles of *Colq*$^{-/-}$ mice rescues AChE activity and ColQ in the noninjected triceps where they are colocalized to acetylcholine receptors (AChR). Bar = 10 µm. (**b**) The size of ColQ-positive area is normalized for the size of AChR-positive area at the neuromuscular junctions (NMJs) of noninjected triceps. (**c**) Signal intensities of ColQ at the NMJs of noninjected triceps. Mean and SE are indicated. WT, wild-type mice, number of NMJs = 43; Protein injected, mice injected with ColQ-tailed AChE, number of NMJs = 42. *$P < 0.001$. Signal intensities are normalized to that of *Colq*$^{-/-}$ mice. Quantitative analyses were performed with the BZ-9000 microscope and the Dynamic Cell Count software BZ-H1C (Keyence).

with deficit in AChE. We observed ColQ-tailed AChE at all of the NMJs examined and the amount of the anchored AChE reached 89.3% of the wild-type level. The improved motor functions lasted at least 48 weeks after treatment and the treated mice survived 18–20 months, which is in contrast to at most 6-month lifespan of *Colq*$^{-/-}$ mice.[12] Although >99.5% of the vector genome stays episomal in mouse muscles even at 57 weeks after injection,[20,21] expression of the transgene in skeletal muscle lasts for 1.0–1.5 years without a decline in immunocompetent mice.[22,23] Our studies also underscore the long-lasting expression of the transgene delivered by AAV.

Rat *Colq*[24] and human *COLQ*[7] have two distinct promoters and generate ColQ1 and ColQ1a transcripts, which respectively include exon 1 and exon 1a and encode distinct signal peptides. A nerve-derived factor, calcitonin gene-related peptide, controls the expression of ColQ1a at the NMJs of fast-twitch muscles. However, in slow-twitch muscles, expression of ColQ1 occurs throughout the muscle fibers and is controlled by Ca^{2+}/calmodulin-dependent protein kinase II and myocyte enhancer factor 2.[24,25] As our viral construct was driven by the cytomegalovirus promoter, spatial and temporal regulation of ColQ expression should have been lost. In addition, our construct expressed ColQ1 and not ColQ1a, which was expected to be physiological for slow-twitch muscle but not for fast-twitch muscles. The prominent ultrastructural improvement in slow-twitch muscles rather than fast-twitch muscles may be partly because AAV8-*COLQ* encodes ColQ1 and not ColQ1a. This also suggests that the N-termini of ColQ1 and 1a have different functions. The pattern of ColQ expression resulting from our strategy was not physiological in three ways: (i) lack of subsynaptic nuclei-specific expression of ColQ, (ii) a ubiquitous cytomegalovirus promoter, and (iii) the exclusive expression of ColQ1. Despite these features, the motor and the synaptic functions are improved; AChE is locally accumulated at the NMJ in our treated mice. This suggests that the precise genetic control of the expression of ColQ is not the key factor for clustering of AChE and tissue-targeting signals of ColQ are sufficient to functionally restore AChE at the NMJ.

The protein-anchoring therapy

Although ColQ-tailed AChE in the serum of either wild type, *Colq*$^{-/-}$, or treated mice was less than a detection threshold in the

sedimentation analysis (**Supplementary Figure S1d–f**), anchoring of ColQ-tailed AChE to remote NMJs was supported by two lines of evidence: local intramuscular injections of AAV1-*COLQ-IRES-EGFP* (**Figure 6**) and of the purified recombinant ColQ-tailed AChE protein complex (**Figure 7**). In either case, AChE at the NMJ of the noninjected muscle originates from ColQ-tailed AChE arising from another source; not from local secretion and retention of ColQ-tailed AChE synthesized by subsynaptic nuclei followed by assembly and maturation in the postsynaptic area as in wild-type mice. The overlay of recombinant ColQ-tailed AChE *in vitro* either on normal muscle tissue sections of frog[5,18] or of *Colq*$^{-/-}$ mouse (**Supplementary Figure S2**) demonstrates that ColQ harbors a signal that targets AChE to the NMJ. The dual interactions of ColQ with MuSK[6] and perlecan,[5] which are both required in the overlay experiment,[18] are likely to restrict ColQ to the NMJ. In endplate AChE deficiency, point mutations that affect the binding of ColQ to MuSK prevent the accumulation of AChE.[18] Although no mutation has been reported at the heparan sulfate proteoglycan-binding domains of ColQ in endplate AChE deficiency, the reduction of perlecan mimicking Schwartz–Jampel syndrome reduces the level of AChE and ColQ at the NMJ.[26,27] All of these observations suggest that the combination of MuSK and perlecan determines the number of ColQ-tailed AChE anchored at the NMJ. This notion was previously termed as "molecular parking lots" by Rotundo and colleagues.[28]

ColQ-tailed AChE is a nanostructure made of a rigid collagen of 50-nm length and three AChE tetramers. ColQ-tailed AChE is apparently able to move from one muscle to another as demonstrated by clustering in the triceps muscle after protein injection into the gluteus. A similar approach is inherently employed by nature, as exemplified by fibronectin that is ubiquitously present in extracellular matrices and is largely derived from liver.[29] Injection of a protein complex is reported with laminin-111.[30] An intramuscularly or intraperitoneally injected laminin-111 is distributed to the basal lamina of skeletal and cardiac muscles in an mdx-mouse model of Duchenne muscular dystrophy. In contrast to our strategy, laminin-111 is not expressed or accumulated in normal or dystrophic adult muscles. Their studies exploit an ectopic deposition of laminin-111 to induce expression of α_7-integrin that stabilizes the sarcolemma of dystrophic muscle fibers.

The ColQ must be synthesized in cells that produce a splice variant T of AChE for obtaining the correct assembly of the complex.[2] A single muscle fiber harbors hundreds of nuclei that are functionally compartmentalized, and a molecule expressed in a single nucleus goes through the muscle fiber only for a short distance.[31,32] Thus, the multinucleation of muscle fibers is unlikely to have contributed to the restoration of function in the *Colq*$^{-/-}$ mice of our study. Similar specific clustering of a muscle-generated protein to the NMJ has been reported with laminin β2.[33] When laminin β2 is expressed throughout muscle fibers by the MCK promoter in transgenic mice, it is clustered at the NMJ.

The inability to achieve efficient and specific delivery of a transgene to the target tissue often prevents the application of gene therapy to model animals and patients.[34] Here, we propose the protein-anchoring strategy that provides a new therapeutic approach for congenital defects of extracellular matrix proteins.[35] The potential candidate molecules of the protein-anchoring therapy include laminin α2 causing laminin-α2-deficient congenital muscular dystrophy,[36] perlecan causing Schwartz–Jampel syndrome,[26,37] and collagen VI causing Ullrich syndrome.[38] It should be emphasized that this strategy can be potentially used for a huge number of diseases caused by mutations of genes encoding proteins of the extracellular matrices in general.

MATERIALS AND METHODS

Preparation of AAV carrying COLQ. Human *COLQ* cDNA[7] was cloned into pAAV-MCS (AAV Helper-Free system; Stratagene, Santa Clara, CA) that carries the cytomegalovirus promoter to obtain a pAAV-*COLQ*. We also inserted *IRES-EGFP* to make pAAV-*COLQ-IRES-EGFP*. To make AAV8-*COLQ*, HEK293 cells were cotransfected with the following plasmids: the proviral vector plasmid pAAV-*COLQ*, the AAV8 chimeric helper plasmid pRC8, and the adenoviral helper plasmid pHelper (Stratagene) using calcium phosphate coprecipitation method.[39] To make AAV1-*COLQ-IRES-EGFP*, we transfected HEK293 cells with pAAV-*COLQ-IRES-EGFP*, the AAV1 chimeric helper plasmid pRep2Cap1, and pHelper. The AAV particles were concentrated by CsCl gradient ultracentrifugation for 3 hours[40] and further purified with the quick dual ion-exchange procedures.[41] The viral titer was estimated by quantitative PCR in real-time using MX3000p (Stratagene).[42]

Administration of AAV carrying COLQ to Colq$^{-/-}$ mice. All animal studies were approved by the Animal Care and Use Committee of the Nagoya University Graduate School of Medicine. For intravenous administration, 1×10^{11}–2×10^{12} vg of AAV8-*COLQ* were injected into the tail vein of 4-week-old *Colq*$^{-/-}$ mice.[12] For intramuscular administration, 2×10^{11} vg of AAV1-*COLQ-IRES-EGFP* were injected into the left anterior tibial muscle of 4-week-old *Colq*$^{-/-}$ mice. The left proximal thigh was tightly ligated with a tourniquet for 20 minutes during intramuscular injection to prevent vascular delivery of viral particles throughout the body.

Motor activity tests. Muscle weakness and fatigability were measured with a rotarod apparatus (Ugo, Basile, Italy). Mice were first trained three times to be accommodated to the task. Mice were consecutively examined three times and were allowed to take a rest for 1 hour between individual tasks.

Running-wheel activity was used to quantify voluntary exercises. Each mouse was placed in a standard cage equipped with a counter-equipped running wheel (diameter, 14.7 cm, width, 5.2 cm; Ohara Medical, Tokyo, Japan). The running distances were recorded using the counter every 24 hours.

Histology. We raised a polyclonal ColQ antibody by injecting a synthetic peptide of SAALPSLDQKKRGGHKAC, corresponding to codons 34–51 in human ColQ, into rabbits. We confirmed that the raised antibody recognized ColQ by western blotting (**Supplementary Figure S3**) and that no signal was present in a section of *Colq*$^{-/-}$ mice (**Figure 4b** and **Supplementary Figure S2**). Mice were sacrificed at 6 weeks after treatment. Skeletal muscles of mice were frozen in the liquid nitrogen-cooled isopentane and sectioned at 8-μm thick with a Leica CW3050-4 cryostat at −20 °C. Muscle sections were blocked with 5% horse serum in phosphate-buffered saline for 20 minutes and incubated with the primary antibody (1:100) for 2 hours. Sections were then incubated with a secondary antibody (1:100) for 1 hour, along with Alexa-594-conjugated α-bungarotoxin (2.5 μg/ml) (Sigma, St Louis, MO) for visualizing AChR. Anti-rabbit and anti-mouse secondary antibodies were both FITC-labeled (Vector Lab, Burlingame, CA). For AAV1-*COLQ-IRES-EGFP*, we detected ColQ using anti-rabbit secondary antibody labeled with rhodamine (1:40; Santa Cruz, Santa Cruz, CA) and localized AChR by Alexa-647-conjugated α-bungarotoxin (2.5 μg/ml; Sigma). Signals of ColQ, AChE, AChR, and EGFP were examined with BX60 (Olympus, Tokyo, Japan) or BZ-9000 (Keyence, Osaka, Japan).

Mouse AChE activity was detected by the histochemical method at 6 weeks after treatment. Muscle sections were incubated for 20 minutes at 37 °C in the reaction mixture containing 1.73 mmol/l acetylthiocholine iodide, 38 mmol/l sodium acetate, 51 mmol/l acetic acid, 6 mmol/l sodium

citrate, 4.7 mmol/l copper sulfate, 0.5 mmol/l potassium ferricyanide, and 5×10^{-5} mol/l ethopropazine (Sigma), which is an inhibitor of butyrylcholinesterase.

Sedimentation biochemical analyses. Mice were sacrificed at 6 weeks after treatment. Sedimentation analysis was performed as previously described.[7] Proteins were extracted from the muscle and liver in a detergent buffer [10 mmol/l HEPES (pH 7.2), 1% CHAPS, 10 mmol/l EDTA, 2 mmol/l benzamidine, leupeptin (20 μg/ml) and pepstatin (10 μg/ml)] containing 0.8 mol/l NaCl. The eluate was applied on a 5–20% sucrose density gradient, which was made in the detergent buffer containing 0.8 mol/l NaCl, along with β-galactosidase (16S) and alkaline phosphatase (6.1S) as internal sedimentation standards. Centrifugation was performed in a Beckman SW41Ti rotor at 4 °C for 21 hours at 38,000 r.p.m. AChE activity was assayed by the colorimetric method of Ellman in the presence of 5×10^{-5} mol/l ethopropazine.

For biochemical analysis, skeletal muscle was shattered by the Cool Mill (Toyobo, Osaka, Japan) in liquid nitrogen. We extracted globular forms of AChE into the NaCl-free detergent buffer, and ColQ-tailed AChE into detergent buffer containing 0.8 mol/l NaCl as previously described.[12] AChE activity was assayed using AChE-Specific Assay kit (Dojindo, Kumamoto, Japan) or the Ellman method and normalized by Torpedo AChE activity (Sigma).

Microelectrode studies. Phrenic nerve-diaphragm preparations were obtained from three wild type, three *Colq*$^{-/-}$, and three AAV8-*COLQ*-treated mice at 8 weeks of age, which corresponds to 4 weeks after treatment. We stimulated the sciatic nerve at 2 Hz and recorded compound muscle action potentials of gastrocnemius muscles using a needle electrode under deep anesthesia. For technical reasons, we could not analyze the limb muscles that we used in the other assays. After mice were sacrificed, miniature endplate potentials and evoked EPPs were recorded as described elsewhere.[43] Neostigmine methylsufate (Elkins-Sinn, Cherry Hill, NJ) was used at a concentration of 10^{-6} g/ml in the bath to block cholinesterases. We employed the AxoGraph × 1.1.6 (AxoGraph Scientific, Sydney, Australia) for data analysis.

Electron microscopy. For electron microscopy, extensor digitorum longus and soleus muscles were fixed in ice-cold 3% glutaraldehyde buffered with 0.1 mol/l cacodylate buffer (pH 7.3) at 4 weeks after treatment. The endplate-rich region of the muscle was refixed in 2% OsO_4 in cacodylate buffer, dehydrated, and embedded in Epon812.

All thin sections were cut transversely, stained with lead citrate, and photographed in a JEM 1,200 EX electron microscopy. Morphometric analysis of the motor endplate was performed following the procedure of Engel and Santa,[44] and included the following: (i) presynaptic membrane length, in μm; (ii) nerve terminal area, in μm^2; (iii) number of synaptic vesicles per unit area, in numbers per μm^2; (iv) length of processes of Schwann cells on presynaptic membrane, in μm; (v) percentage of totally enwrapped nerve terminal by processes of Schwann cells; (vi) postsynaptic area of folds and clefts associated with a given nerve terminal, in μm^2; (vii) postsynaptic membrane length associated with a given nerve terminal, in μm; (viii) postsynaptic membrane length per unit postsynaptic area (postsynaptic membrane density), derived by dividing the value of (vii) by that of (vi), in μm per μm^2; (ix) postsynaptic to presynaptic membrane ratio. Endplates were localized and analyzed by established methods, and peroxidase-labeled α-bungarotoxin was used for the ultrastructural localization of AChR.[45] The images were quantified using the NIH Image 1.62 software (National Institutes of Health).

Expression and purification of recombinant ColQ. The plasmids that previously introduced human *COLQ* and human *ACHE* cDNAs into a pTargeT (Promega, Madison, WI)[7] were cotransfected into HEK293 cells. Proteins were extracted from the cells in Tris–HCl buffer [50 mmol/l Tris–HCl (pH 7.0), 0.5% Triton X-100, 0.2 mmol/l EDTA, leupeptin (2 μg/ml), and pepstatin (1 μg/ml)] containing 1 mol/l NaCl. The extracts were loaded onto HiTrap Heparin HP columns (GE Healthcare, Buckinghamshire, UK). The concentration of purified recombinant ColQ-tailed AChE was equivalent to ~4 μg/ml Torpedo AChE. We injected 50 μl of the purified ColQ-tailed AChE in phosphate-buffered saline daily into the gluteus maximus muscles of 5-week-old *Colq*$^{-/-}$ mice for a week. Mice were given a single intraperitoneal injection of 300 mg/kg cyclophosphamide monohydrate (10 mg/ml in saline) at 24 hours after the first ColQ-tailed AChE injection to suppress immunoreaction against the recombinant human protein.[46] After 7 days, mice were sacrificed and brachial muscles were stained for ColQ molecule and AChE activity as described above.

Real-time PCR/reverse transcription-PCR. For expression analysis, total RNAs from skeletal muscle and liver cells were extracted using the RNeasy Mini kit (Qiagen, Hilden, Germany) with *DNaseI* and proteinase K treatment according to the manufacturer's instructions. First-stranded cDNA was synthesized using the ReverTra Ace reverse transcriptase (Toyobo). Expressions of human *COLQ*, mouse *Colq*, and mouse *Ache* were analyzed using the TaqMan (Applied Biosystems, Foster city, CA) probes and primers in LightCycler 480 (Roche, Mannheim, Germany). We also quantified 18S rRNA for normalization.

To quantify the transduction efficiency, total DNA was extracted from skeletal muscle and liver using the QIAamp DNA Mini Kit (Qiagen). The amount of viral genome was quantified by real-time PCR using a TaqMan probe targeting to human *COLQ*, as well as to mouse *Tert* encoding telomerase reverse transcriptase to normalize for the cell numbers.

SUPPLEMENTARY MATERIAL

Figure S1. Sedimentation analyses of AChE in the liver and serum.
Figure S2. Binding of human ColQ-tailed AChE proteins to the NMJ in muscle section of *Colq*$^{-/-}$ mice.
Figure S3. Western blot of a newly raised rabbit polyclonal anti-ColQ antibody (1:1,000).
Table S1. Morphometric analysis of endplate ultrastructures.
Video 1. First part: Two *Colq*$^{-/-}$ mice treated with an intravenous administration of 2×10^{12} vg of AAV8-*COLQ* (right cage) move around actively.

ACKNOWLEDGMENTS

We thank James M. Wilson for providing the chimeric helper plasmid pRC8 (identical to p5E18-VD2/8) and pRep2Cap1 (identical to p5E18RXCl). This work was supported by Grants-in-Aid from the Ministry of Education, Culture, Sports, Science, and Technology of Japan, and the Ministry of Health, Labor, and Welfare of Japan, as well as by Grant from ANR maladies rares. The authors declared no conflict of interest.

REFERENCES

1. Krejci, E, Thomine, S, Boschetti, N, Legay, C, Sketelj, J and Massoulié, J (1997). The mammalian gene of acetylcholinesterase-associated collagen. *J Biol Chem* **272**: 22840–22847.
2. Rotundo, RL (1984). Asymmetric acetylcholinesterase is assembled in the Golgi apparatus. *Proc Natl Acad Sci USA* **81**: 479–483.
3. Ruiz, CA and Rotundo, RL (2009). Limiting role of protein disulfide isomerase in the expression of collagen-tailed acetylcholinesterase forms in muscle. *J Biol Chem* **284**: 31753–31763.
4. Deprez, P, Inestrosa, NC and Krejci, E (2003). Two different heparin-binding domains in the triple-helical domain of ColQ, the collagen tail subunit of synaptic acetylcholinesterase. *J Biol Chem* **278**: 23233–23242.
5. Peng, HB, Xie, H, Rossi, SG and Rotundo, RL (1999). Acetylcholinesterase clustering at the neuromuscular junction involves perlecan and dystroglycan. *J Cell Biol* **145**: 911–921.
6. Cartaud, A, Strochlic, L, Guerra, M, Blanchard, B, Lambergeon, M, Krejci, E *et al.* (2004). MuSK is required for anchoring acetylcholinesterase at the neuromuscular junction. *J Cell Biol* **165**: 505–515.
7. Ohno, K, Brengman, J, Tsujino, A and Engel, AG (1998). Human endplate acetylcholinesterase deficiency caused by mutations in the collagen-like tail subunit (ColQ) of the asymmetric enzyme. *Proc Natl Acad Sci USA* **95**: 9654–9659.
8. Donger, C, Krejci, E, Serradell, AP, Eymard, B, Bon, S, Nicole, S *et al.* (1998). Mutation in the human acetylcholinesterase-associated collagen gene, COLQ, is responsible

for congenital myasthenic syndrome with end-plate acetylcholinesterase deficiency (Type Ic). *Am J Hum Genet* **63**: 967–975.
9. Ohno, K, Engel, AG, Brengman, JM, Shen, XM, Heidenreich, F, Vincent, A *et al.* (2000). The spectrum of mutations causing end-plate acetylcholinesterase deficiency. *Ann Neurol* **47**: 162–170.
10. Bestue-Cardiel, M, Sáenz de Cabezón-Alvarez, A, Capablo-Liesa, JL, López-Pisón, J, Peña-Segura, JL, Martin-Martinez, J *et al.* (2005). Congenital endplate acetylcholinesterase deficiency responsive to ephedrine. *Neurology* **65**: 144–146.
11. Mihaylova, V, Müller, JS, Vilchez, JJ, Salih, MA, Kabiraj, MM, D'Amico, A *et al.* (2008). Clinical and molecular genetic findings in COLQ-mutant congenital myasthenic syndromes. *Brain* **131**(Pt 3): 747–759.
12. Feng, G, Krejci, E, Molgo, J, Cunningham, JM, Massoulié, J and Sanes, JR (1999). Genetic analysis of collagen Q: roles in acetylcholinesterase and butyrylcholinesterase assembly and in synaptic structure and function. *J Cell Biol* **144**: 1349–1360.
13. Lee, HH, Choi, RC, Ting, AK, Siow, NL, Jiang, JX, Massoulié, J *et al.* (2004). Transcriptional regulation of acetylcholinesterase-associated collagen ColQ: differential expression in fast and slow twitch muscle fibers is driven by distinct promoters. *J Biol Chem* **279**: 27098–27107.
14. Ruiz, CA and Rotundo, RL (2009). Dissociation of transcription, translation, and assembly of collagen-tailed acetylcholinesterase in skeletal muscle. *J Biol Chem* **284**: 21488–21495.
15. Inagaki, K, Fuess, S, Storm, TA, Gibson, GA, Mctiernan, CF, Kay, MA *et al.* (2006). Robust systemic transduction with AAV9 vectors in mice: efficient global cardiac gene transfer superior to that of AAV8. *Mol Ther* **14**: 45–53.
16. Nakai, H, Fuess, S, Storm, TA, Muramatsu, S, Nara, Y and Kay, MA (2005). Unrestricted hepatocyte transduction with adeno-associated virus serotype 8 vectors in mice. *J Virol* **79**: 214–224.
17. Bouma, SR, Drislane, FW and Huestis, WH (1977). Selective extraction of membrane-bound proteins by phospholipid vesicles. *J Biol Chem* **252**: 6759–6763.
18. Kimbell, LM, Ohno, K, Engel, AG and Rotundo, RL (2004). C-terminal and heparin-binding domains of collagenic tail subunit are both essential for anchoring acetylcholinesterase at the synapse. *J Biol Chem* **279**: 10997–11005.
19. Wang, Z, Zhu, T, Qiao, C, Zhou, L, Wang, B, Zhang, J *et al.* (2005). Adeno-associated virus serotype 8 efficiently delivers genes to muscle and heart. *Nat Biotechnol* **23**: 321–328.
20. Schnepp, BC, Clark, KR, Klemanski, DL, Pacak, CA and Johnson, PR (2003). Genetic fate of recombinant adeno-associated virus vector genomes in muscle. *J Virol* **77**: 3495–3504.
21. Kay, MA (2007). AAV vectors and tumorigenicity. *Nat Biotechnol* **25**: 1111–1113.
22. Xiao, X, Li, J and Samulski, RJ (1996). Efficient long-term gene transfer into muscle tissue of immunocompetent mice by adeno-associated virus vector. *J Virol* **70**: 8098–8108.
23. Rivière, C, Danos, O and Douar, AM (2006). Long-term expression and repeated administration of AAV type 1, 2 and 5 vectors in skeletal muscle of immunocompetent adult mice. *Gene Ther* **13**: 1300–1308.
24. Krejci, E, Legay, C, Thomine, S, Sketelj, J and Massoulié, J (1999). Differences in expression of acetylcholinesterase and collagen Q control the distribution and oligomerization of the collagen-tailed forms in fast and slow muscles. *J Neurosci* **19**: 10672–10679.
25. Lau, FT, Choi, RC, Xie, HQ, Leung, KW, Chen, VP, Zhu, JT *et al.* (2008). Myocyte enhancer factor 2 mediates acetylcholine-induced expression of acetylcholinesterase-associated collagen ColQ in cultured myotubes. *Mol Cell Neurosci* **39**: 429–438.
26. Arikawa-Hirasawa, E, Rossi, SG, Rotundo, RL and Yamada, Y (2002). Absence of acetylcholinesterase at the neuromuscular junctions of perlecan-null mice. *Nat Neurosci* **5**: 119–123.
27. Stum, M, Girard, E, Bangratz, M, Bernard, V, Herbin, M, Vignaud, A *et al.* (2008). Evidence of a dosage effect and a physiological endplate acetylcholinesterase deficiency in the first mouse models mimicking Schwartz-Jampel syndrome neuromyotonia. *Hum Mol Genet* **17**: 3166–3179.
28. Rotundo, RL, Rossi, SG and Anglister, L (1997). Transplantation of quail collagen-tailed acetylcholinesterase molecules onto the frog neuromuscular synapse. *J Cell Biol* **136**: 367–374.
29. Moretti, FA, Chauhan, AK, Iaconcig, A, Porro, F, Baralle, FE and Muro, AF (2007). A major fraction of fibronectin present in the extracellular matrix of tissues is plasma-derived. *J Biol Chem* **282**: 28057–28062.
30. Rooney, JE, Gurpur, PB and Burkin, DJ (2009). Laminin-111 protein therapy prevents muscle disease in the mdx mouse model for Duchenne muscular dystrophy. *Proc Natl Acad Sci USA* **106**: 7991–7996.
31. Hall, ZW and Ralston, E (1989). Nuclear domains in muscle cells. *Cell* **59**: 771–772.
32. Rossi, SG, Vazquez, AE and Rotundo, RL (2000). Local control of acetylcholinesterase gene expression in multinucleated skeletal muscle fibers: individual nuclei respond to signals from the overlying plasma membrane. *J Neurosci* **20**: 919–928.
33. Miner, JH, Go, G, Cunningham, J, Patton, BL and Jarad, G (2006). Transgenic isolation of skeletal muscle and kidney defects in laminin beta2 mutant mice: implications for Pierson syndrome. *Development* **133**: 967–975.
34. Somia, N and Verma, IM (2000). Gene therapy: trials and tribulations. *Nat Rev Genet* **1**: 91–99.
35. Mueller, C and Flotte, TR (2008). Clinical gene therapy using recombinant adeno-associated virus vectors. *Gene Ther* **15**: 858–863.
36. Helbling-Leclerc, A, Zhang, X, Topaloglu, H, Cruaud, C, Tesson, F, Weissenbach, J *et al.* (1995). Mutations in the laminin alpha 2-chain gene (LAMA2) cause merosin-deficient congenital muscular dystrophy. *Nat Genet* **11**: 216–218.
37. Nicole, S, Davoine, CS, Topaloglu, H, Cattolico, L, Barral, D, Beighton, P *et al.* (2000). Perlecan, the major proteoglycan of basement membranes, is altered in patients with Schwartz-Jampel syndrome (chondrodystrophic myotonia). *Nat Genet* **26**: 480–483.
38. Kawahara, G, Okada, M, Morone, N, Ibarra, CA, Nonaka, I, Noguchi, S *et al.* (2007). Reduced cell anchorage may cause sarcolemma-specific collagen VI deficiency in Ullrich disease. *Neurology* **69**: 1043–1049.
39. Okada, T, Nomoto, T, Yoshioka, T, Nonaka-Sarukawa, M, Ito, T, Ogura, T *et al.* (2005). Large-scale production of recombinant viruses by use of a large culture vessel with active gassing. *Hum Gene Ther* **16**: 1212–1218.
40. Okada, T, Shimazaki, K, Nomoto, T, Matsushita, T, Mizukami, H, Urabe, M *et al.* (2002). Adeno-associated viral vector-mediated gene therapy of ischemia-induced neuronal death. *Meth Enzymol* **346**: 378–393.
41. Okada, T, Nonaka-Sarukawa, M, Uchibori, R, Kinoshita, K, Hayashita-Kinoh, H, Nitahara-Kasahara, Y *et al.* (2009). Scalable purification of adeno-associated virus serotype 1 (AAV1) and AAV8 vectors, using dual ion-exchange adsorptive membranes. *Hum Gene Ther* **20**: 1013–1021.
42. Rohr, UP, Wulf, MA, Stahn, S, Steidl, U, Haas, R and Kronenwett, R (2002). Fast and reliable titration of recombinant adeno-associated virus type-2 using quantitative real-time PCR. *J Virol Methods* **106**: 81–88.
43. Engel, AG, Nagel, A, Walls, TJ, Harper, CM and Waisburg, HA (1993). Congenital myasthenic syndromes: I. Deficiency and short open-time of the acetylcholine receptor. *Muscle Nerve* **16**: 1284–1292.
44. Engel, AG and Santa, T (1971). Histometric analysis of the ultrastructure of the neuromuscular junction in myasthenia gravis and in the myasthenic syndrome. *Ann N Y Acad Sci* **183**: 46–63.
45. Engel, AG, Lindstrom, JM, Lambert, EH and Lennon, VA (1977). Ultrastructural localization of the acetylcholine receptor in myasthenia gravis and in its experimental autoimmune model. *Neurology* **27**: 307–315.
46. Otterness, IG and Chang, YH (1976). Comparative study of cyclophosphamide, 6-mercaptopurine, azathiopurine and methotrexate. Relative effects on the humoral and the cellular immune response in the mouse. *Clin Exp Immunol* **26**: 346–354.

NUCLEIC ACID THERAPEUTICS
Volume 22, Number 5, 2012

DOI: 10.1089/nat.2012.0368

Extensive and Prolonged Restoration of Dystrophin Expression with Vivo-Morpholino-Mediated Multiple Exon Skipping in Dystrophic Dogs

Toshifumi Yokota,[1–3] Akinori Nakamura,[3,4] Tetsuya Nagata,[3] Takashi Saito,[3,5] Masanori Kobayashi,[3,6] Yoshitsugu Aoki,[3] Yusuke Echigoya,[1] Terence Partridge,[7,8] Eric P. Hoffman,[7,8] and Shin'ichi Takeda[3]

Duchenne muscular dystrophy (DMD) is a severe and the most prevalent form of muscular dystrophy, characterized by rapid progression of muscle degeneration. Antisense-mediated exon skipping is currently one of the most promising therapeutic options for DMD. However, unmodified antisense oligos such as morpholinos require frequent (weekly or bi-weekly) injections. Recently, new generation morpholinos such as vivo-morpholinos are reported to lead to extensive and prolonged dystrophin expression in the dystrophic *mdx* mouse, an animal model of DMD. The vivo-morpholino contains a cell-penetrating moiety, octa-guanidine dendrimer. Here, we sought to test the efficacy of multiple exon skipping of exons 6–8 with vivo-morpholinos in the canine X-linked muscular dystrophy, which harbors a splice site mutation at the boundary of intron 6 and exon 7. We designed and optimized novel antisense cocktail sequences and combinations for exon 8 skipping and demonstrated effective exon skipping in dystrophic dogs *in vivo*. Intramuscular injections with newly designed cocktail oligos led to high levels of dystrophin expression, with some samples similar to wild-type levels. This is the first report of successful rescue of dystrophin expression with morpholino conjugates in dystrophic dogs. Our results show the potential of phosphorodiamidate morpholino oligomer conjugates as therapeutic agents for DMD.

Introduction

DUCHENNE MUSCULAR DYSTROPHY (DMD) is a lethal and the most common form of muscular dystrophy worldwide, which affects 1 in 3,500 boys (Duchenne, 1867; Zellweger and Antonik, 1975). There is currently no effective cure for DMD. Most patients die in their 20s–30s with respiratory or heart failure. DMD and its milder form, Becker muscular dystrophy, are caused by mutations in the *dystrophin* (*DMD*) gene (Hoffman et al., 1987; Koenig et al., 1987). Antisense oligonucleotide-mediated exon skipping therapy is a most promising approach to curing DMD (Pramono et al., 1996; Dunckley et al., 1998; Goyenvalle et al., 2011; Lu et al., 2011). Antisense oligos such as phosphorodiamidate morpholino oligomers (PMOs, or morpholinos) and 2'O- methyl antisense oligos with phosphorothioate bonds (2'OMePS) against dystrophin mRNA lead to the production of internally deleted in-frame transcripts both *in vitro* and *in vivo* (Pramono et al., 1996; Dunckley et al., 1998; Lu et al., 2005; Yokota et al., 2009a; Yokota et al., 2012). The truncated quasi-dystrophin retains some functions like mild Becker dystrophy or even leads to asymptomatic individuals in some cases (Beroud et al., 2006; Nakamura et al., 2008; Aoki et al., 2010; Goyenvalle et al., 2010). Exon skipping therapies with PMO or 2'OMePS

[1]Department of Medical Genetics, School of Human Development, Faculty of Medicine and Dentistry, University of Alberta, Edmonton, Alberta, Canada.
[2]The Friends of Garrett Cumming Research & Muscular Dystrophy Canada HM Toupin Neurological Science Research Chair, Edmonton, Alberta, Canada.
[3]Department of Molecular Therapy, National Institute of Neuroscience, National Center of Neurology and Psychiatry (NCNP), Tokyo, Japan.
[4]Third Department of Internal Medicine, Shinshu University School of Medicine, Matsumoto, Japan.
[5]Department of Pediatrics, School of Medicine, Tokyo Women's Medical University, Tokyo, Japan.
[6]Department of Reproduction, Nippon Veterinary and Life Science University, Tokyo, Japan.
[7]Research Center for Genetic Medicine, Children's National Medical Center, Washington, District of Columbia.
[8]Department of Integrative Systems Biology, George Washington University School of Medicine, Washington, District of Columbia.

antisense oligos targeting the exon 51 are currently under phase-2/3 clinical trials (Aartsma-Rus and van Ommen, 2007; van Deutekom et al., 2007; Kinali et al., 2009; Cirak et al., 2011; Goemans et al., 2011).

One of the biggest challenges of exon-skipping therapy is that the single exon skipping is applicable to only approximately 50% of DMD patients (total of each single individual target exon). In contrast, double or multiple exon skipping is potentially applicable to 90% of patients (Aartsma-Rus et al., 2006; Yokota et al., 2007a). The dystrophic dog requires more than one exon skipping (multiple exon skipping targeting exon 6 and exon 8 in the dystrophin mRNA). Previously we reported the first successful multiple (double) exon-skipping treatment in body-wide skeletal muscles in Canine X-linked muscular dystrophy (CXMD) with a cocktail of antisense phosphorodiamidate morpholino oligomers (PMOs, morpholinos) (Yokota et al., 2009a). The dog trial targeting exon 6 and exon 8 of dystrophin mRNA led to 27% normal levels of dystrophin expression in body-wide skeletal muscles detected by western blotting analysis on average. However, unmodified morpholinos exhibit inefficient long-term delivery. The half-life of dystrophin expression was approximately 1–2 months (Wu et al., 2010).

Recently, new generation morpholinos such as cell-penetrating peptide conjugated phosphorodiamidate morpholino oligomers (PPMOs) and vivo-morpholinos (vPMOs) were reported to induce prolonged and extensive rescue of dystrophin expression and ameliorate the function in cardiac muscles in dystrophic *mdx* mice (Wu et al., 2009; Goyenvalle et al., 2010; Jearawiriyapaisarn et al., 2010; Crisp et al., 2011; Widrick et al., 2011; Wu et al., 2011a). vPMOs are morpholino oligomers conjugated with delivery moiety containing eight terminal guanidinium groups on a dendrimer scaffold that enable entry into cells (Fig. 1A) (Morcos et al., 2008). New generation morpholinos are efficiently delivered into various tissues including muscle fibers *in vivo* (Wu et al., 2009). Vivo-morpholino-mediated splice modulation efficiently also rescued Fukuyama congenital muscular dystrophy model mice and primary myotubes from human patients (Taniguchi-Ikeda et al., 2011). Their delivery efficacy is reported to be more than 50 times higher than unmodified morpholinos (Wu et al., 2009).

In this study, we focused on 2 aims. First, we employed a novel backbone (vivo-morpholino) for the antisense therapy in the dog model. Second, we tested novel antisense oligo cocktails designed for multiple exon skipping (exons 6 and 8) in the canine *DMD* gene. We hypothesized that (1) vivo-morpholinos induce extensive and prolonged dystrophin expression in dystrophic dogs, and (2) our novel antisense oligo cocktail can improve the efficacy of exon 6–8 multiple skipping. We tested these hypotheses and the efficacy of multiple (double) exon skipping in dystrophic dogs *in vivo*. Vivo-morpholinos with newly optimized sequences induced near normal level of dystrophin protein and prolonged expression recovery.

Materials and Methods

Ethics Statement

All animal works have been conducted according to relevant national and international guidelines. The Experimental Animal Care and Use Committee of the National Institute of Neuroscience, National Center of Neurology and Psychiatry (NCNP) Japan approved all experimental protocols in this study. We obtained consent from all of the owners of the dogs involved in this study (All dogs are owned by NCNP).

Animals

The CXMD dog is the beagle dog model of DMD (Shimatsu et al., 2003). They were allowed *ad libitum* access to food and drinking water. Dogs carrying mutations were identified by reverse-transcription polymerase chain reaction (RT-PCR) analysis as previously described (Sharp et al., 1992). Three- to five-month-old dogs were used. Five dystrophic dogs were used for injections. Four dystrophic dogs and three wild-type dogs were used as non-treated controls. Animals were euthanized by exsanguination under general anesthesia.

Antisense oligos

Antisense oligos for targeted skipping of exons 6 and exon 8 in the canine *DMD* gene were used as previously described (Tables 1, 2) (Yokota et al., 2009a; Saito et al., 2010). All PMOs and vPMOs were obtained from Gene-tools, Inc (Morcos et al., 2008). As control oligos, we employed Ex6A only (GTTGATTGTCGGACCCAGCTCAGG) or 3-oligo cocktail containing Ex6A (GTTGATTGTCGGACCCAGCTCAGG), Ex6B (ACCTATGACTGTGGATGAGAGCGTT), and Ex8A (CTTCCTGGATGGCTTCAATGCTCAC) for intramuscular injections as indicated. The dose selection is based on previous mouse studies with PMOs and vPMOs, showing that vPMOs induce more than 10×higher efficacy, and dog studies with PMOs (Wu et al., 2009). The Ex8G dose and ratio were determined based on previous cell experiments (Saito et al., 2010).

Injections

Animals were anesthetized with thiopental sodium induction and maintained by isoflurane (Nacalai Tesque, Inc.) for all intramuscular injections and muscle biopsies. General anesthesia was maintained with isoflurane administered through an endotracheal tube. Skin was excised over the site of injection, muscle exposed, and the injection site marked with a suture in the muscle. Antisense oligonucleotides were delivered by intramuscular injection using 1 mL saline bolus into indicated skeletal muscles using a 27-gauge needle. Antisense oligonucleotides were delivered as a singular or in mixtures as previously described (Yokota et al., 2011). Tibialis anterior, extensor digitorum longus, extensor carpi ulnaris, flexor digitorum superficialis (FDS), flexor carpi ulnaris (FCU), and flexor carpi radialis (FCR) muscles were used for injections. Muscles samples were obtained 2 or 8 weeks after the intramuscular injections. Muscles were obtained immediately, snap-frozen in liquid nitrogen–cooled isopentane, and stored at −80°C for immunohistochemistry and western blotting. Skeletal muscle tissues were cut and collected in microtubes and snap-frozen in liquid nitrogen for RT-PCR analysis.

Immunohistochemical analysis

Antibodies. The following monoclonal antibodies were used for immunofluorescence: anti-dystrophin DYS-1 (Novocastra, Newcastle upon Tyne, UK). Alexa 488, or Alexa 594 conjugated goat anti mouse secondary antibodies (Invitrogen).

Immunofluorescence. Cryosections (7.5 μm) were blocked with 20% goat serum in phosphate buffered saline,

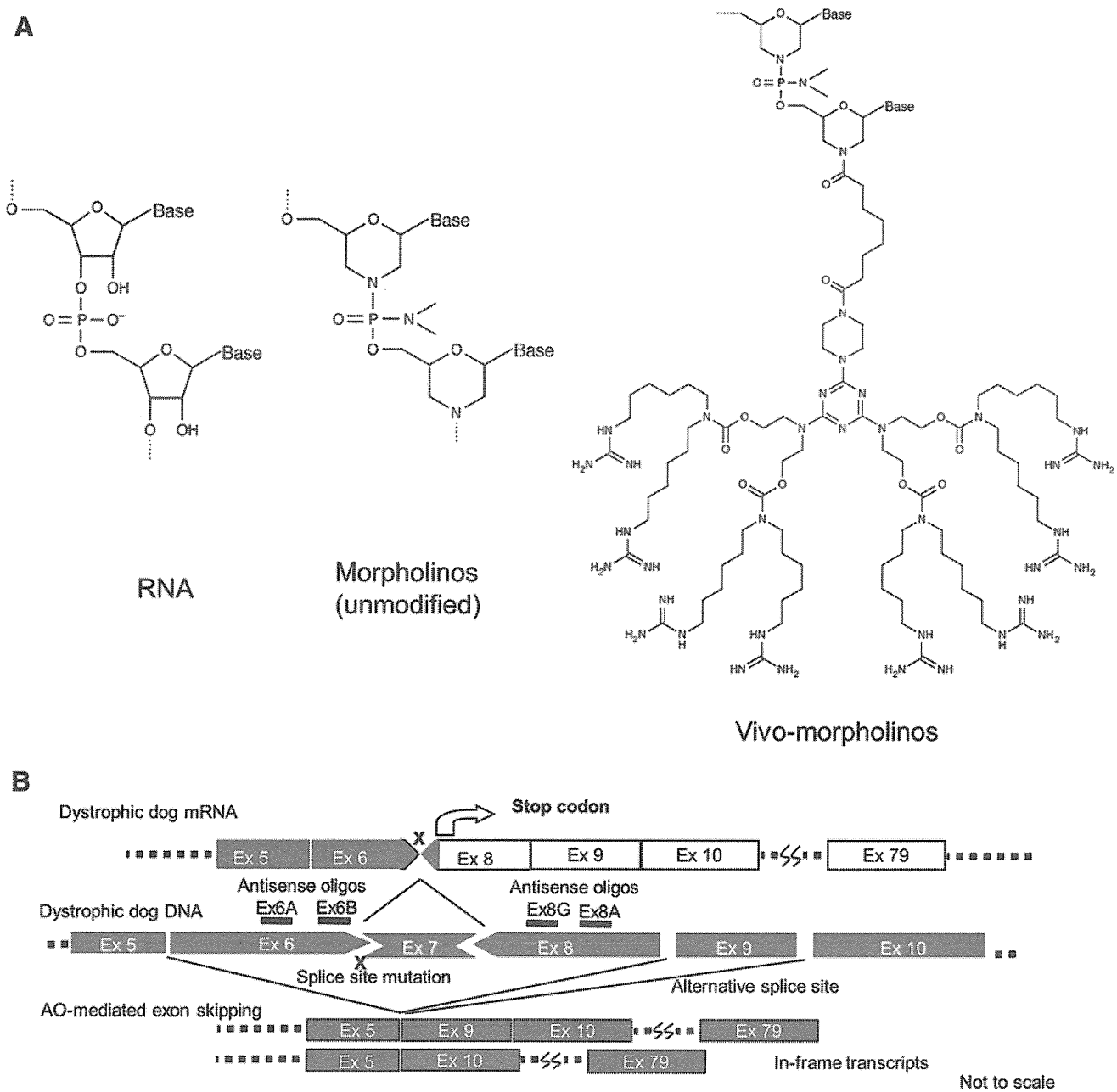

FIG. 1. Antisense chemistry and design of multiple exon skipping for dystrophic dogs. **(A)** Comparison of antisense oligos. **(B)** Schematic design of multi (double) exon skipping therapy for dystrophic dogs. At least two exons (exons 6 and 8) need to be skipped (removed) with antisense oligos to correct their reading frame. Gua, Guanidine.

and then incubated with a primary antibody at 4°C overnight. Alexa 488, or 594-conjugated anti-mouse goat antibody (Invitrogen, Camarillo, CA) was used as the secondary antibody. The sections were viewed and photographed by a laser scanning microscope, FluoView™ (Olympus, Tokyo, Japan) The number of positive fibers for DYS-1 was counted and compared in sections containing the largest number of positive fibers as described previously (Yokota et al., 2006). At least 200 muscle fibers were counted in each section for the analysis.

TABLE 1. ANTISENSE OLIGO SEQUENCES

Oligo name	*Sequence (5′–3′)*
Ex6A	GTTGATTGTCGGACCCAGCTCAGG
Ex6B	ACCTATGACTGTGGATGAGAGCGTT
Ex8A	CTTCCTGGATGGCTTCAATGCTCAC

TABLE 2. ADDITIONAL ANTISENSE OLIGO SEQUENCES FOR EXON 8

Oligo name	*Sequence (5′–3′)*
Ex8G	GGCAAAACTTGGAAGAGTGATGTGA
Ex8I	CCTTGGCAACATTTCCACTTCCTGG
Ex8K	TTTACCTGTTGAGAATAGTGCATTT

Western blotting analysis

Muscle proteins from cryosections were extracted with lysis buffer containing 75 mM Tris-HCl (pH 6.8), 10% sodium dodecyl sulfate, 10 mM EDTA, and 5% 2-mercaptoethanol. Four to 40 μg proteins were loaded onto precase 3%–8% resolving sodium dodecyl sulfate polyacrylamide gel electrophoresis gels following manufacturer's instructions (Bio-Rad, Hercules, CA). The gels were transferred by semidry blotting at 400 mA for 1.5 hours. DYS-1 (Novocastra) antibody against dystrophin and rabbit polyclonal antibody against desmin (Abcam) were used as primary antibodies. Horseradish peroxidase–conjugated anti-mouse or anti-rabbit goat immunoglobulin (Cedarlane Laboratories, Hornby, Ontario,

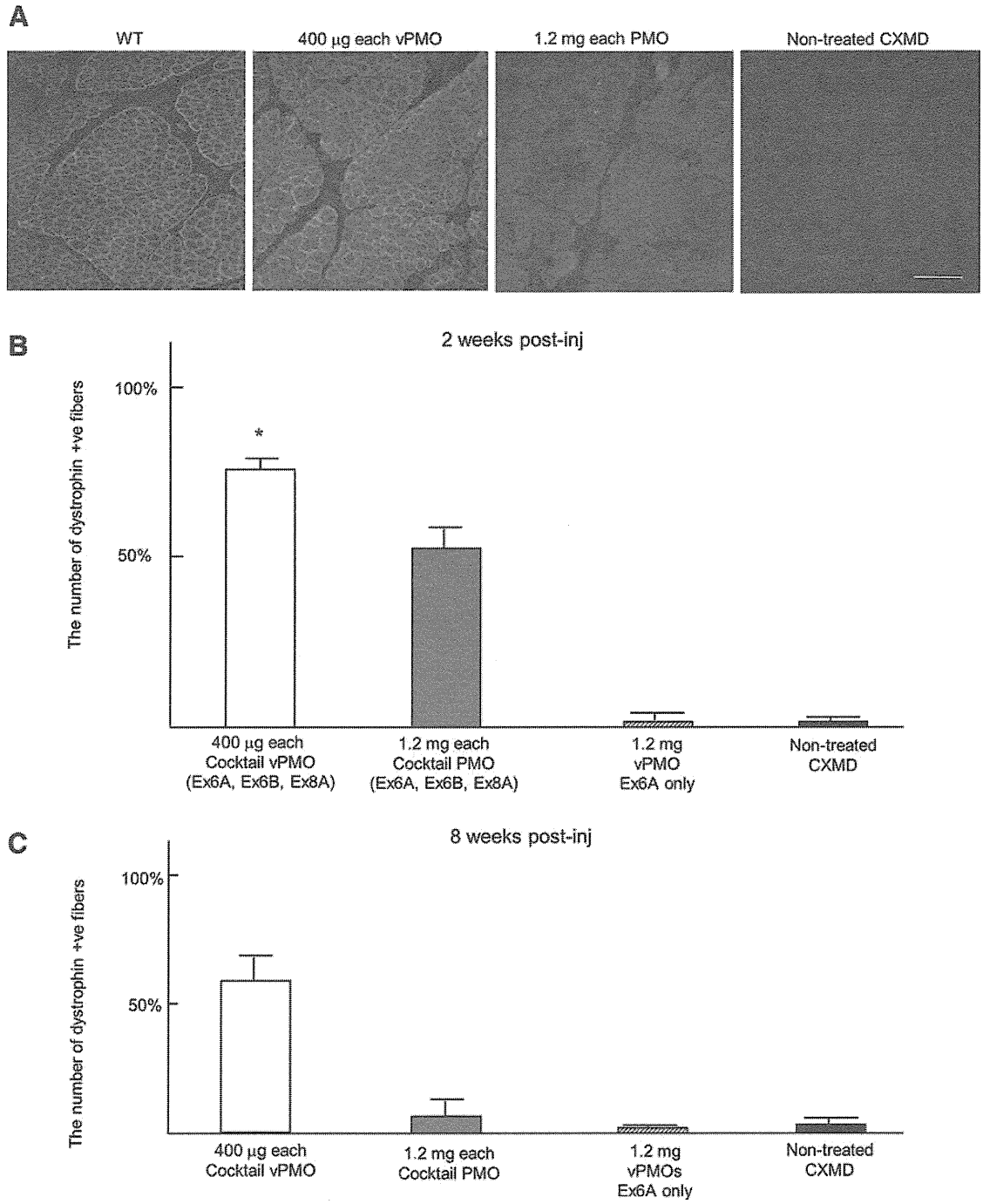

FIG. 2. Vivo phosphorodiamidate morpholino oligomer (vPMO) local injections restore dystrophin expression in TA 8 weeks later. **(A)** Immunohistochemistry with dystrophin (DYS1) antibody 8 weeks after the cocktail vPMO treatment containing Ex6A, Ex6B, and Ex8A in canine X-linked muscular dystrophy (CXMD) (1.2 mg in total as a cocktail, 400 μg of each oligo), and unmodified morpholino treatment containing Ex6A, Ex6B, and Ex8A in CXMD (3.6 mg in total as a cocktail, 1.2 mg of each oligo). **(B)** The number of dystrophin positive fibers 2 weeks after injections. **(C)** The number of dystrophin positive fibers 8 weeks after injections. Scale bar = 200 μm; n = 2–4 in each group; $^*P < 0.05$ compared with non-treated control group.

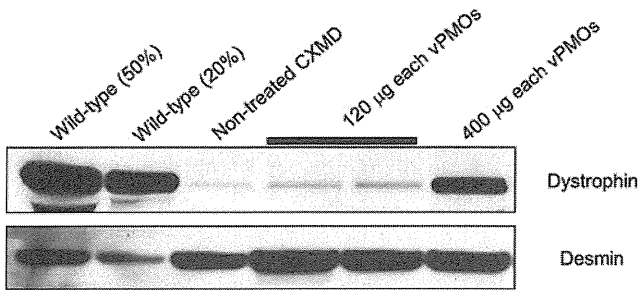

FIG. 3. Prolonged dystrophin expression after vPMO injections. Western blotting analysis on dystrophin expression with DYS-1 antibody 8 weeks after vPMO cocktail injections (120 μg each or 400 μg each of Ex6A, Ex6B, and Ex8A) into TA muscles in dystrophic dogs as indicated.

Canada) was used as a secondary antibody. Enzyme chemiluminescence kit (GE, Fairfield, CT) was used for the detection. Blots were analyzed by ImageJ software (Collins, 2007).

Reverse transcriptase polymerase chain reaction

Total RNA was extracted from frozen tissue sections using TRIzol (Invitrogen). Then RT-PCR was performed on 200 ng of total RNA for 35 cycles of amplification using One-Step RT-PCR kit (Qiagen, Chatsworth, CA) following manufacturer's instructions with 0.6 μM of an exon 5 (CTGACTCTTGGTTTGATTTGGA) forward primer. Reverse primers were exon 10 (TGCTTCGGTCTCTGTCAATG).

Statistical analysis

The data between samples were compared using *F*-test and Student's or Welch's *t*-test. $P<0.05$ was considered statistically significant.

Results

Design of antisense vivo-morpholinos

In this study, we employed a cocktail of antisense vivo-morpholino oligos (Gene-tools) to induce exon skipping of exon 6 and exon 8 in the canine *dystrophin* (*DMD*) gene (Fig. 1A). A vivo-morpholino is comprised of a morpholino oligo with a covalently linked delivery moiety, an octa-guanidine dendrimer. As previously demonstrated, at least two exons (exon 6 and exon 8) need to be removed to restore the reading frame of the splice site mutation in the CXMD (Fig. 1B) (McClorey et al., 2006; Yokota et al., 2009a). Initially, we employed a cocktail oligo with the same sequences and combinations, Ex6A, Ex6B, and Ex8A, as previously used (Yokota et al., 2009a) (Table 1). We compared the efficacy of exon skipping by vPMOs and unmodified morpholinos.

Sustained dystrophin expression after cocktail vPMO injections

Since sustained recovery of dystrophin expression was previously reported after vivo-morpholino injections into dystrophic *mdx* mice, we tested the dystrophin expression levels 2 weeks and 8 weeks after vPMO injections in cranial tibialis (tibialis anterior in humans) muscles in dystrophic dogs (Fig. 2) (Jearawiriyapaisarn et al., 2008; Wu et al., 2009; Widrick et al., 2011; Wu et al., 2011a). In this study, we employed 3- to 5-month-old dystrophic dogs. At this stage the disease progression was relatively mild in these dogs. We employed a cocktail of three antisense oligos named Ex6A, Ex6B, and Ex8A (Table 1). We used anti-rod domain dystrophin antibody because anti-C-terminus dystrophin antibodies cross-react with other dystrophin isoforms (e.g., Dp71).

While unmodified PMO (1.2 mg each, or 3.6 mg in total as a cocktail) injected muscle showed almost no detectable dystrophin expression 8 weeks after injections, extensive dystrophin expression was observed after 400 μg vPMO injected muscles (Fig. 2A). At 2 weeks after the vPMO (400 μg each) injection, approximately 75% of fibers were positive with dystrophin DYS-1 antibody, while 55% were positive after unmodified PMO injection (1.2 mg each) (Fig. 2B). A cocktail of antisense vPMOs was required to induce dystrophin expression (Fig.2B). Injections with single antisense vPMO targeting exon 6 only (Ex6A) did not induce detectable level of dystrophin expression (Fig. 2B). At 8 weeks after vPMO injection, approximately 60% of fibers were still positive with DYS-1 antibody, while only 10% were positive after unmodified PMO injection (Fig. 2C).

The expression level of dystrophin was then examined by western blotting analysis (Fig. 3). Approximately 20% of the level of dystrophin in wild-type was detected in vPMO-injected muscles 8 weeks after the injection with 400 μg each of Ex6A, Exx6B, and Ex8A (or 1.2 mg in total as a cocktail).

Design of novel antisense sequences and combinations for dystrophin exon 8

Next, to further optimize the antisense oligo sequences and combinations, we tested new oligos named Ex8G, Ex8I, and Ex8K (Fig. 4, Table 2). In previous study, these oligos

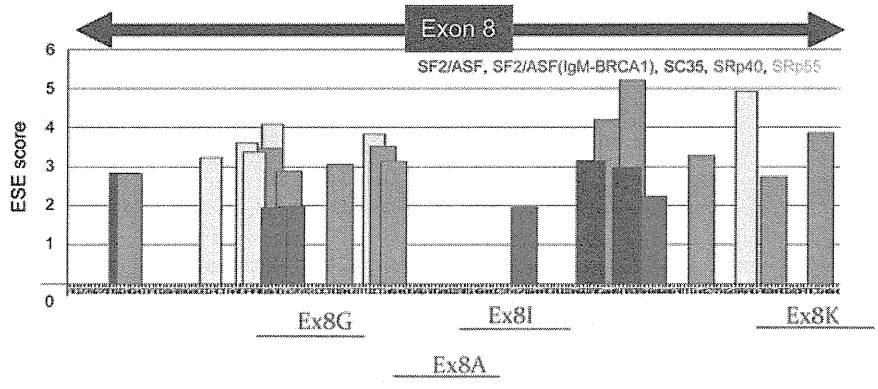

FIG. 4. Schematic outline of the antisense morpholinos targeting exon 8 of dog and human dystrophin mRNA. Antisense oligos against exon 8 of human/dog *DMD* gene used in this study. These 4 oligos were previously reported to be effective for exon 8 skipping in myotubes of dystrophic dogs and human patients *in vitro* (Saito et al., 2010).

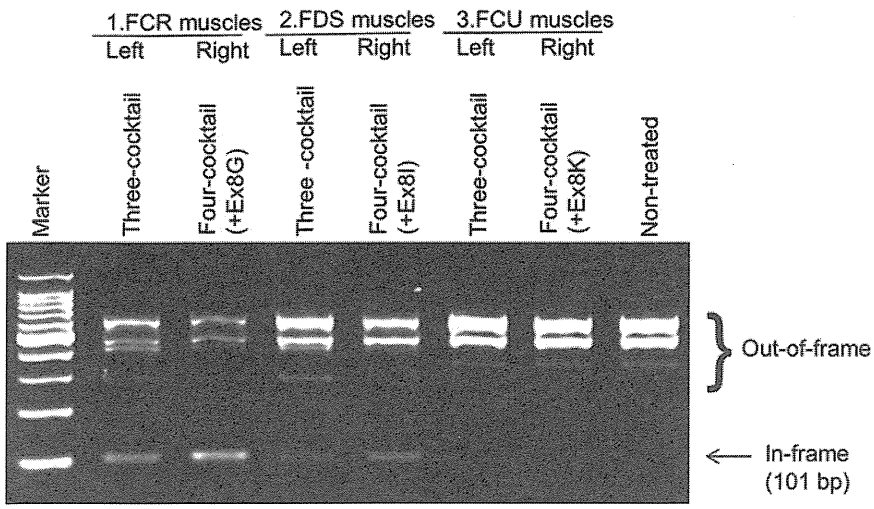

FIG. 5. A 4-oligo cocktail containing Ex8G induces efficient dystrophin expression. Detection of exon 6–9 skipped band with reverse-transcription polymerase chain reaction analysis. Equal amounts (120 μg) of oligos in total were injected into indicated muscles (i.e., 40 μg each in three-oligo cocktails, 30 μg each in four-oligo cocktails). FCR, flexor carpi radialis; FDS, flexor digitorum superficialis; FCU, flexor carpi ulnaris.

efficiently induced exon 8 skipping *in vitro* in dog and human myotubes (Saito et al., 2010). These oligos were designed to target exon/intron borders or exonic splice enhancer (ESE) sites. ESE scores were obtained by using ESE finder software (Cartegni et al., 2003). These oligos target the same conserved sequences in both dog and human dystrophin mRNA.

A novel antisense cocktail induces more efficient exon 8 skipping

We tested the efficacy of newly designed oligos by intramuscular injections into skeletal muscles in dystrophic dogs (Fig. 5). We previously reported a cocktail oligo containing Ex6A, Ex6B, Ex8A, and Ex8G led to the most efficient double exon skipping of exon 6–8 (or triple skipping of exon 6–9) in both human and dog myotubes *in vitro* (Saito et al., 2010). Exon 9 was not targeted by antisense oligos but the exon is known as an alternative splice site which is spontaneously skipped with exon 6–8 skipping induced by antisense oligos in previous studies (Reiss and Rininsland 1994; McClorey et al., 2006). Here, we compared the efficacy of multiple exon skipping induced by the three oligos cocktail which we have previously reported effective for systemic trials in dystrophic dogs (Yokota et al., 2009a), and newly designed 4-oligo cocktails, which we found to be more effective *in vitro* (Saito et al., 2010). Here, 3-oligo cocktail oligos (Ex6A + Ex6B + Ex8A) were injected into right-side muscles of flexor carpi radialis (FCR), Flexor digitorum superficialis (FDS), or flexor carpi ulnaris (FCU) as controls. Different combinations of 4-oligo cocktails were injected into contralateral (left side) muscles (Fig. 5). The same total doses (120 μg) of 3-oligo cocktails or of 4-oligo cocktails were injected (i.e., 40 μg each in 3-oligo cocktails, and 30 μg each in 4-oligo cocktails). The efficacy of multiple exon skipping was initially examined by RT-PCR analysis. While all combinations led to substantial amount of exon 6–9 skipped in-frame mRNA products, the highest efficacy was achieved with the 4-oligo cocktail containing Ex8G (Ex6A + Ex6B + Ex8A + Ex8G), which is consistent with our previous report in myotubes *in vitro* (Saito et al., 2010).

Efficient dystrophin recovery after injections with four-oligo cocktail vPMOs

Next, we examined the recovery of dystrophin expression by immunohistochemistry with DYS-1 anti-dystrophin monoclonal antibody 2 weeks after intramuscular vPMO injections (Fig. 6). Although all tested cocktail oligos induced extensive expression of dystrophin, the highest recovery was obtained with the 4-oligo cocktail containing Ex6A, Ex6B, Ex8A, and Ex8G (Fig. 6). Approximately 70 percent of fibers was positively stained with the four-oligo cocktail (Fig. 6B).

The expression levels of dystrophin after cocktail vPMO injections were also compared with western blotting analysis (Fig. 7). Desmin antibody was used as an internal control. Again, the 4-oligo cocktail injection with Ex6A, Ex6B, Ex8A, and Ex8G led to the highest levels of dystrophin expression.

Discussion

Antisense mediated exon skipping is currently a most promising therapeutic approach to curing DMD (Yokota et al., 2007b; Hoffman et al., 2011; Partridge 2011; Pichavant et al., 2011). Although phase-2/3 clinical trials are currently underway, there are a couple of challenges. One of the most significant challenges is that the effect usually wears off after 3–4 weeks, thus repeated injections are required. Currently, weekly or bi-weekly injections are required for antisense systemic trials (Lu et al., 2005; Alter et al., 2006; Wu et al., 2011b). New generation morpholinos with cell-penetrating moiety, such as PPMOs and vPMOs, were developed to improve the efficacy *in vivo* (Moulton and Jiang 2009; Yokota et al., 2009b). Both PPMOs and vPMOs have the same backbones as conventional unmodified morpholinos (Fig. 1). In vPMOs, cell-penetrating octa-guanidine dendrimers are conjugated, while in PPMOs, arginine rich polypeptides are conjugated (Morcos et al., 2008). Peptide-morpholino conjugates (PPMOs) restored dystrophin to more than 80 percent of wild-type levels in skeletal muscles of *mdx* mice 9 weeks after injections, showing prolonged activity (Moulton et al., 2009). An injection with vPMOs in hDMD mice, a transgenic model carrying the full-length human dystrophin gene, led to more than 70% efficiency of targeted human dystrophin exon skipping *in vivo* systemically (Wu et al., 2011a). Therefore, use of morpholino conjugates such as PPMOs or vPMOs might be able to reduce the frequency of injections.

In this study, we demonstrated the first successful rescue of dystrophin expression with morpholino conjugates in dystrophic dogs. In previous *in vitro* experiments, we used a total

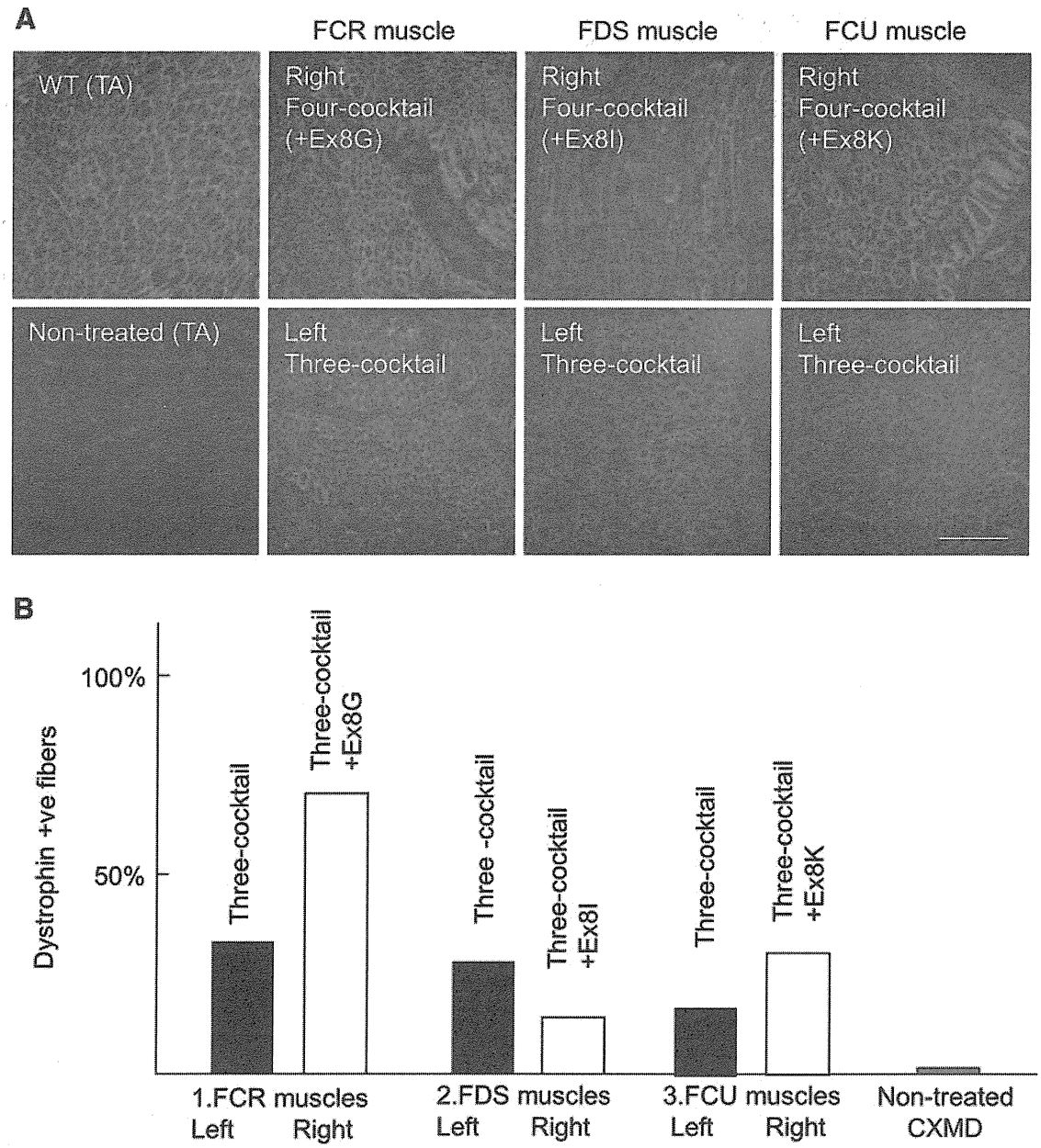

FIG. 6. Immunohistochemistry shows four-oligo cocktails induce efficient dystrophin expression *in vivo*. **(A)** Immunohistochemistry with anti-dystrophin antibody (DYS-1; red) and DAPI nuclei staining (blue). Equal amounts (120 μg) of oligos in total were injected into indicated muscles (i.e., 40 μg each in 3-oligo cocktails, 30 μg each in 4-oligo cocktails). Scale bars = 200 μm. **(B)** The percentage of dystrophin positive fibers after cocktail oligo injections.

of 30 μM for 3 or 4 sequences of PMOs (Saito et al., 2010). In this study, we employed 120μg–1.2 mg of vPMOs for intramuscular injections. The induction of exon 6–9 multiple skipping mediated by cocktail vPMOs was significantly more efficient than that mediated by unconjugated PMOs (Fig. 2). The expression levels were remained very high (60% dystrophin-positive fibers) 2 months after the injection, indicating prolonged persistence (Figs. 2–3). We employed dogs in early stages of the disease, because muscle fibers are replaced by fibrous connective tissue at later stages. This might be generalized to the antisense drug products intended for use in the first-in-human trial. Importantly, a vPMO cocktail efficiently rescued other genetic disorders including the mutation in Fukuyama congenital muscular dystrophy (Taniguchi-Ikeda et al., 2011). These studies clearly indicate that morpholino conjugates are not only useful tools for gene-knockdown study, but also have great potential for treating genetic disorders.

We next compared newly designed antisense oligos against exon 8 of dystrophin mRNA *in vivo* (Figs. 5–7). In accordance with the previous study *in vitro* by Saito et al., the most efficient vPMO cocktail was a 2 oligo cocktail containing Ex8A and Ex8G (Saito et al., 2010). Since exon 6, 7, and 8 are all among the most prevalent targets of exon skipping therapy outside the deletion mutation hotspot (exon 45–55), optimization of antisense oligos against these exons is very

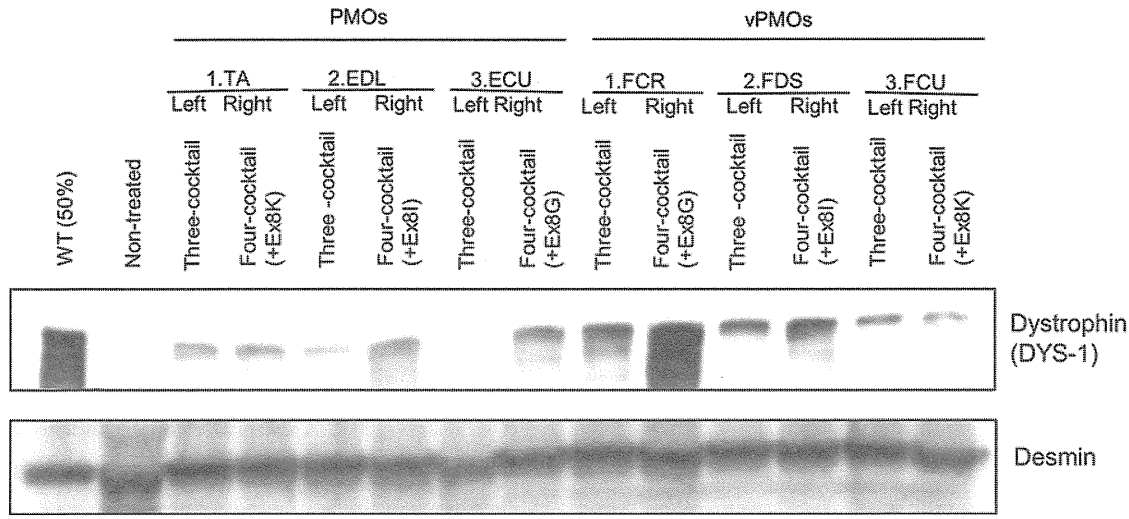

FIG. 7. Restoration of dystrophin expression with f4-oligo cocktail vPMOs. Western blotting analysis with anti-dystrophin (DYS-1) antibody 2 weeks after vPMO injections. Equal amounts (120 μg) of oligos in total were injected into indicated muscles (i.e., 40 μg each in 3-oligo cocktails, 30 μg each in 4-oligo cocktails). The 4-oligo cocktail (Ex6A + Ex6B + Ex8A + Ex8G) leads to the highest level of dystrophin expression. TA, tibialis anterior; EDL, extensor digitorum longus; ECU, extensor carpi ulnaris.

important. In fact, approximately 3.0% of DMD patients can be treated with double skipping of exon 6 and exon 7 (ranked No. 9), and 2.3% can be treated with skipping exon 8 (ranked No. 10) (Aartsma-Rus et al., 2009). Because the exon-skipping approach is fundamentally a mutation-specific personalized medicine, an effective path of drug approval process will be also a key to rescue mutations with a relatively small number of patients.

A major concern of new generation morpholino-mediated antisense therapy is their toxicity. No toxicity of vPMOs has been recorded up to 12 mg/kg of systemic injections in mice (Wu et al., 2009). However, with PPMOs, a high dose (150 mg/kg) of systemic injections led to adverse events such as lethargy, weight loss, elevated blood urea nitrogen, and serum creatinine levels (Amantana et al., 2007). In addition, a test in the cynomolgus monkey revealed mild tubular degeneration in the kidneys after weekly injections with 9 mg/kg PPMOs (Moulton and Moulton, 2010). Although AVI-5038, a PPMO targeting exon 50 of dystrophin mRNA, is in preclinical development, the toxicity of PPMOs might pose a challenge for determination of an effective and safe regimen in man. An immune suppression regimen such as one used for robust adeno-associated virus expression might be effective for systemic trials (Shin et al., 2012; Wang et al., 2007). To test the systemic effect of vPMOs in dogs, precise pharmacokinetics, biodistribution, stability, and toxicity remain to be done. Nevertheless, our results indicate clear potential of the morpholino conjugate as a therapeutic agent to treat DMD and other genetic disorders.

Acknowledgments

We thank Michihiro Imamura, Jing Hong Shin, Takashi Okada, Michiko Wada, Sachiko Ohshima, Jun Tanihata, Satoru Masuda, Kazue Kinoshita, Hideki Kita, Shinichi Ichikawa, Yumiko Yahata, Yuko Kasahara, and Yuko Shimizu (NCNP); and Merryl Rodriguez and Dharminder Panesar (University of Alberta) for useful discussions and technical assistance. This work was supported by Grants-in-Aid for Research on Nervous and Mental Disorders (19A-7), Health and Labor Sciences Research Grants for Translation Research (H19-Translational Research-003 and H21-Clinical Research-015), and Health Sciences Research Grants for Research on Psychiatry and Neurological Disease and Mental Health (H18-kokoro-019) from the Ministry of Health, Labour, and Welfare of Japan, U.S. National Institutes of Health (1P50AR060836; 5T32AR056993), US Department of Defense (W81XWH-09-1-0599) The Friends of Garrett Cumming Research, HM Toupin Neurological Science Research, and Muscular Dystrophy Canada.

TY, TS, AN, and ST conceived and designed study. TY, AN, MK, and TS performed experiments. ST, EH, TN, YA, YO, YE and TP analyzed the data. TY, YA, and TS contributed reagents/materials/analysis tools. TY wrote the manuscript.

Author Disclosure Statement

No competing financial interests exist.

References

AARTSMA-RUS, A., FOKKEMA, I., VERSCHUUREN, J., GINJAAR, I., et al. (2009). Theoretic applicability of antisense-mediated exon skipping for Duchenne muscular dystrophy mutations. Hum. Mutat. **30,** 293–299.

AARTSMA-RUS, A., KAMAN, W.E., WEIJ, R., DEN DUNNEN, J.T., et al. (2006). Exploring the frontiers of therapeutic exon skipping for Duchenne muscular dystrophy by double targeting within one or multiple exons. Mol. Ther. **14,** 401–407.

AARTSMA-RUS, A., and VAN OMMEN, G.J. (2007). Antisense-mediated exon skipping: A versatile tool with therapeutic and research applications. RNA **13,** 1609–1624.

ALTER, J., LOU, F., RABINOWITZ, A., YIN, H., et al. (2006). Systemic delivery of morpholino oligonucleotide restores dystrophin expression bodywide and improves dystrophic pathology. Nat. Med. **12,** 175–177.

AMANTANA, A., MOULTON, H.M., CATE M.L., REDDY M.T., et al. (2007). Pharmacokinetics, biodistribution, stability and toxicity of a cell-penetrating peptide-morpholino oligomer conjugate. Bioconjug. Chem. **18,** 1325–1331.

AOKI, Y., NAKAMURA, A., YOKOTA, T., SAITO, T., et al. (2010). In-frame dystrophin following exon 51-skipping improves muscle pathology and function in the exon 52-deficient mdx mouse. Mol. Ther. **18,** 1995–2005.

BEROUD, C., TUFFERY-GIRAUD, S., MATSUO, M., HAMROUN, D., et al. (2006). Multiexon skipping leading to an artificial DMD protein lacking amino acids from exons 45 through 55 could rescue up to 63% of patients with Duchenne muscular dystrophy. Hum. Mutat. **28,** 196–202.

CARTEGNI, L., WANG, J., ZHU, Z., ZHANG, M.Q., et al. (2003). ESEfinder: A web resource to identify exonic splicing enhancers. Nucleic Acids Res. **31,** 3568–3571.

CIRAK, S., ARECHAVALA-GOMEZA, V., GUGLIERI, M., FENG, L., et al. (2011). Exon skipping and dystrophin restoration in patients with Duchenne muscular dystrophy after systemic phosphorodiamidate morpholino oligomer treatment: an open-label, phase 2, dose-escalation study. Lancet **378,** 595–605.

COLLINS, T.J. (2007). ImageJ for microscopy. Biotechniques 43, 25–30.

CRISP, A., YIN, H., GOYENVALLE, A., BETTS, C., et al. (2011). Diaphragm rescue alone prevents heart dysfunction in dystrophic mice. Hum. Mol. Genet. **20,** 413–421.

DUCHENNE. (1867). The pathology of paralysis with muscular degeneration (paralysie myosclerotique), or paralysis with apparent hypertrophy. Br. Med. J. **2,** 541–542.

DUNCKLEY, M.G., MANOHARAN, M., VILLIET, P., EPERON, I.C., et al. (1998). Modification of splicing in the dystrophin gene in cultured Mdx muscle cells by antisense oligoribonucleotides. Hum. Mol. Genet. **7,** 1083–1090.

GOEMANS, N.M., TULINIUS, M., VAN DEN AKKER, J.T., BURM, B.E., et al. (2011). Systemic administration of PRO051 in Duchenne's muscular dystrophy. N. Engl. J. Med. **364,** 1513–1522.

GOYENVALLE, A., BABBS, A., POWELL, D., KOLE, R., et al. (2010). Prevention of dystrophic pathology in severely affected dystrophin/utrophin-deficient mice by morpholino-oligomer-mediated exon-skipping. Mol. Ther. **18,** 198–205.

GOYENVALLE, A., SETO, J.T., DAVIES, K.E., and CHAMBERLAIN, J. (2011). Therapeutic approaches to muscular dystrophy. Hum. Mol. Genet. **20,** R69–78.

HOFFMAN, E.P., BRONSON, A., LEVIN, A.A., TAKEDA, S., et al. (2011). Restoring dystrophin expression in Duchenne muscular dystrophy muscle progress in exon skipping and stop codon read through. Am. J. Pathol. **179,** 12–22.

HOFFMAN, E.P., BROWN, R.H., JR., and KUNKEL, L.M. (1987). Dystrophin: the protein product of the Duchenne muscular dystrophy locus. Cell **51,** 919–928.

JEARAWIRIYAPAISARN, N., MOULTON, H.M., BUCKLEY, B., ROBERTS, J., et al. (2008). Sustained dystrophin expression induced by peptide-conjugated morpholino oligomers in the muscles of mdx mice. Mol. Ther. **16,** 1624–1629.

JEARAWIRIYAPAISARN, N., MOULTON, H.M., SAZANI, P., KOLE, R., et al. (2010). Long-term improvement in mdx cardiomyopathy after therapy with peptide-conjugated morpholino oligomers. Cardiovasc. Res. **85,** 444–453.

KINALI, M., ARECHAVALA-GOMEZA, V., FENG, L., CIRAK, S., et al. (2009). Local restoration of dystrophin expression with the morpholino oligomer AVI-4658 in Duchenne muscular dystrophy: a single-blind, placebo-controlled, dose-escalation, proof-of-concept study. Lancet Neurol. **8,** 918–928.

KOENIG, M., HOFFMAN, E.P., BERTELSON, C.J., MONACO, A.P., et al. (1987). Complete cloning of the Duchenne muscular dystrophy (DMD) cDNA and preliminary genomic organization of the DMD gene in normal and affected individuals. Cell **50,** 509–517.

LU, Q.L., RABINOWITZ, A., CHEN, Y.C., YOKOTA, T., et al. (2005). Systemic delivery of antisense oligoribonucleotide restores dystrophin expression in body-wide skeletal muscles. Proc. Natl. Acad. Sci. U. S. A. **102,** 198–203.

LU, Q.L., YOKOTA, T., TAKEDA, S., GARCIA, L., et al. (2011). The status of exon skipping as a therapeutic approach to duchenne muscular dystrophy. Mol. Ther. **19,** 9–15.

MCCLOREY, G., MOULTON, H.M., IVERSEN, P.L., FLETCHER, S., et al. (2006). Antisense oligonucleotide-induced exon skipping restores dystrophin expression in vitro in a canine model of DMD. Gene Ther. **13,** 1373–1381.1373–1381.

MORCOS, P.A., LI, Y., and JIANG, S. (2008). Vivo-Morpholinos: a non-peptide transporter delivers Morpholinos into a wide array of mouse tissues. Biotechniques **45,** 613–614, 616, 618 passim.

MOULTON, H.M., and MOULTON, J.D. (2010). Morpholinos and their peptide conjugates: therapeutic promise and challenge for Duchenne muscular dystrophy. Biochim. Biophys. Acta **1798,** 2296–2303.

MOULTON, H.M., WU, B., JEARAWIRIYAPAISARN, N., SAZANI, P., et al. (2009). Peptide-morpholino conjugate: a promising therapeutic for Duchenne muscular dystrophy. Ann. N. Y. Acad. Sci. **1175,** 55–60.

MOULTON, J.D., and JIANG, S. (2009). Gene knockdowns in adult animals: PPMOs and vivo-morpholinos. Molecules **14,** 1304–1323.

NAKAMURA, A., YOSHIDA, K., FUKUSHIMA, K., UEDA, H., et al. (2008). Follow-up of three patients with a large in-frame deletion of exons 45–55 in the Duchenne muscular dystrophy (DMD) gene. J. Clin. Neurosci. **15,** 757–763.

PARTRIDGE, T.A. (2011). Impending therapies for Duchenne muscular dystrophy. Curr. Opin. Neurol. **24,** 415–422.

PICHAVANT, C., AARTSMA-RUS, A., CLEMENS, P.R., DAVIES, K.E., et al. (2011). Current status of pharmaceutical and genetic therapeutic approaches to treat DMD. Mol. Ther. **19,** 830–840.

PRAMONO, Z.A., TAKESHIMA, Y., ALIMSARDJONO, H., ISHII, A., et al. (1996). Induction of exon skipping of the dystrophin transcript in lymphoblastoid cells by transfecting an antisense oligodeoxynucleotide complementary to an exon recognition sequence. Biochem. Biophys. Res. Commun. **226,** 445–449.

REISS, J., and RININSLAND, F. (1994). An explanation for the constitutive exon 9 cassette splicing of the DMD gene. Hum. Mol. Genet. **3,** 295–298.

SAITO, T., NAKAMURA, A., AOKI, Y., YOKOTA, T., et al. (2010). Antisense PMO found in dystrophic dog model was effective in cells from exon 7-deleted DMD patient. PLoS One **5,** e12239.

SHARP, N.J., KORNEGAY, J.N., VAN CAMP, S.D., HERBSTREITH, M.H., et al. (1992). An error in dystrophin mRNA processing in golden retriever muscular dystrophy, an animal homologue of Duchenne muscular dystrophy. Genomics **13,** 115–121.

SHIMATSU, Y., KATAGIRI, K., FURUTA, T., NAKURA, M., et al. (2003). Canine X-linked muscular dystrophy in Japan (CXMDJ). Exp. Anim. **52,** 93–97.

SHIN, J.H., YUE, Y., SRIVASTAVA, A., SMITH, B., et al. (2012). A Simplified Immune Suppression Scheme Leads to Persistent

Micro-dystrophin Expression in Duchenne Muscular Dystrophy Dogs. Hum. Gene Ther. **23,** 202–209.

TANIGUCHI-IKEDA, M., KOBAYASHI, K., KANAGAWA, M., YU, C.C., et al. (2011). Pathogenic exon-trapping by SVA retrotransposon and rescue in Fukuyama muscular dystrophy. Nature **478,** 127–131.

VAN DEUTEKOM, J.C., JANSON, A.A., GINJAAR, I.B., FRANKHUIZEN, W.S., et al. (2007). Local dystrophin restoration with antisense oligonucleotide PRO051. N. Engl. J. Med. **357,** 2677–286.

WANG, Z., KUHR, C.S., ALLEN, J.M., BLANKINSHIP, M., et al. (2007). Sustained AAV-mediated dystrophin expression in a canine model of Duchenne muscular dystrophy with a brief course of immunosuppression. Mol. Ther. **15,** 1160–1166.

WIDRICK, J.J., JIANG, S., CHOI, S.J., KNUTH, S.T., et al. (2011). An octaguanidine-morpholino oligo conjugate improves muscle function of mdx mice. Muscle Nerve **44,** 563–570.

WU, B., BENRASHID, E., LU, P., CLOER, C., et al. (2011a). Targeted skipping of human dystrophin exons in transgenic mouse model systemically for antisense drug development. PLoS One **6,** e19906.

WU, B., LI, Y., MORCOS, P.A., DORAN, T.J., et al. (2009). Octa-guanidine morpholino restores dystrophin expression in cardiac and skeletal muscles and ameliorates pathology in dystrophic mdx mice. Mol. Ther. **17,** 864–871.

WU, B., LU, P., BENRASHID, E., MALILK, S., et al. (2010). Dose-dependent restoration of dystrophin expression in cardiac muscle of dystrophic mice by systemically delivered morpholino. Gene Ther. **17,** 132–140.

WU, B., XIAO, B., CLOER, C., SHABAN, M., et al. (2011b). One-year treatment of morpholino antisense oligomer improves skeletal and cardiac muscle functions in dystrophic mdx mice. Mol. Ther. **19,** 576–583.

YOKOTA, T., DUDDY, W., ECHIGOYA, Y., and KOLSKI, H. (2012). Exon skipping for nonsense mutations in Duchenne muscular dystrophy: too many mutations, too few patients? Expert Opin. Biol. Ther.

YOKOTA, T., DUDDY, W., and PARTRIDGE, T. (2007a). Optimizing exon skipping therapies for DMD. Acta Myol. **26,** 179–184. Online document at: http://informahealthcare.com/doi/abs/10.1517/14712598.2012.693469 Accessed June 1, 2012.

YOKOTA, T., HOFFMAN, E.P., and TAKEDA, S. (2011). Antisense oligo-mediated multiple exon skipping in a dog model of Duchenne muscular dystrophy. Methods Mol. Biol. **709,** 299–312.

YOKOTA, T., LU, Q.L., MORGAN, J.E., DAVIES, K.E., et al. (2006). Expansion of revertant fibers in dystrophic mdx muscles reflects activity of muscle precursor cells and serves as an index of muscle regeneration. J. Cell Sci. **119,** 2679–2687.

YOKOTA, T., LU, Q.L., PARTRIDGE, T., KOBAYASHI, M., et al. (2009a). Efficacy of systemic morpholino exon-skipping in Duchenne dystrophy dogs. Ann. Neurol. **65,** 667–676.

YOKOTA, T., PISTILLI, E., DUDDY, W., and NAGARAJU, K. (2007b). Potential of oligonucleotide-mediated exon-skipping therapy for Duchenne muscular dystrophy. Expert Opin. Biol. Ther. **7,** 831–842.

YOKOTA, T., TAKEDA, S., LU, Q.L., PARTRIDGE, T.A., et al. (2009b). A renaissance for antisense oligonucleotide drugs in neurology: exon skipping breaks new ground. Arch. Neurol. **66,** 32–38.

ZELLWEGER, H., and ANTONIK, A. (1975). Newborn screening for Duchenne muscular dystrophy. Pediatrics **55,** 30–34.

Address correspondence to:
Dr. Shin'ichi Takeda, MD, PhD
Department of Molecular Therapy
National Institute of Neuroscience
National Center of Neurology and Psychiatry
Ogawa-higashi 4-1-1
Kodaira, Tokyo 187-8502
Japan

E-mail: takeda@ncnp.go.jp

or

Dr. Toshifumi Yokota, PhD
Department of Medical Genetics
University of Alberta
Faculty of Medicine and Dentistry
8812-112 Street
Edmonton, AB, T6G 2H7
Canada

E-mail: toshifum@ualberta.ca

Received for publication May 17, 2012; accepted after revision July 3, 2012.

Psychiatry and Clinical Neurosciences 2012; **66**: 397–404 doi:10.1111/j.1440-1819.2012.02350.x

Regular Article

Secluded/restrained patients' perceptions of their treatment: Validity and reliability of a new questionnaire

Toshie Noda, MD,[1]* Naoya Sugiyama, MD, PhD,[2] Hiroto Ito, PhD,[1] Päivi Soininen, RN, MSc,[3,4] Hanna Putkonen, MD, PhD,[3] Eila Sailas, MD[3] and Grigori Joffe, MD, PhD[5]

[1]*Department of Social Psychiatry, National Institute of Mental Health, National Center of Neurology and Psychiatry, Kodaira,* [2]*Fukkokai Foundation, Numazu-chuo Hospital, Numazu, Japan,* [3]*Kellokoski Hospital, Kellokoski,* [4]*University of Turk, Turk and* [5]*Helsinki University Central Hospital, Helsinki, Finland*

Aim: To develop a standardized self-reporting questionnaire to evaluate patients' perceptions of their overall treatment in specific relation to the use of seclusion and/or restraint (SR) measures as part of the treatment program.

Methods: A 17-item self-rating questionnaire was given to 56 patients with experience of SR-related treatment to develop a new scale, the Secluded/Restrained Patients' Perceptions of their Treatment (SR-PPT). Concurrent validity was examined against the Client Satisfaction Questionnaire-8 Japanese Version (CSQ-8J). In addition, Patient burden induced by answering the SR-PPT was evaluated.

Results: On factor analysis, two factors named as Cooperation with Staff (nine items) and Perceptions of SR (two items) were derived. Cronbach's coefficient alphas were 0.928 and 0.887, and correlation coefficients against the CSQ-8J were 0.838 and 0.609, respectively. Answering the SR-PPT was found to induce little burden on the patients.

Conclusion: Adequate internal consistency and concurrent validity of the final version of the SR-PPT, which consists of 11 items, indicate that it is acceptable as a measurement scale. Use of this questionnaire will add the patient's view to the assessment of overall treatment involving SR.

Key words: coercion, inpatients, patient participation, patient satisfaction, profession–patient relations.

IN PSYCHIATRIC INPATIENT care, seclusion and/or restraint (SR) is often used to secure the safety of a patient whose disruptive behaviors due to mental disorder pose a potential danger to the patient him/herself and to others in the immediate vicinity, such as patients and care staff.[1] The aims of SR are to ensure a secure environment and to provide medication and care smoothly until SR is no longer considered necessary. It is also reported, however, that patients who have experienced SR felt fear, helplessness and distress. This suggests that they do not consider such intervention beneficial, but rather a form of punishment under the control of care staff.[2–5]

Through various discussions aimed at SR minimization and elimination,[6,7] it has been clarified that the amount of SR in Japan is high compared to other countries. The minimization of SR is an urgent task in Japan.[8] Finland, another country that recognizes itself as a heavy user of SR among European countries, has conducted substantial investigations and has been taking measures for SR minimization.[9,10] From this common awareness, Japan and Finland launched a bilateral project called SAKURA in 2007 to investigate the quality of care involving SR. The project follows the structure, process and outcome proposed by Donabedian[11] and as one of the outcomes, focuses on the evaluation of the patient's own perceptions of his/her treatment.

Correspondence: Toshie Noda, MD, Department of Social Psychiatry, National Institute of Mental Health, National Center of Neurology and Psychiatry, 4-1-1 Ogawa-Higashi, Kodaira, Tokyo 187-8553, Japan. Email: toshie.noda@gmail.com
Received 18 February 2011; revised 27 March 2012; accepted 28 March 2012.

Recent studies have found that patient perception of coercive interventions and/or a weak alliance with care staff lead to poorer adherence to treatment,[12] and that an involuntary admission without understanding the justification for treatment results in a higher rate of readmission.[13] It has been shown that in community mental health care, where patients generally receive treatment at will, closer agreement between the patient's needs and the physician's justification of treatment is associated with a higher level of patient satisfaction and consequently better adherence to the treatment.[14] In addition, the patient's involvement in making treatment decisions improves his/her quality of life (QOL) and satisfaction level.[15,16] Such findings can possibly be extrapolated to patients who have experienced SR, because their perceptions of such treatment and its justification as well as their perceptions of therapeutic collaboration with the staff might influence their prognosis. It is, therefore, necessary for staff providing SR treatment to make efforts to build a therapeutic relationship with the patients, identify their therapeutic needs, and involve them in establishing their own treatment goals. Such tasks are accomplished not only through close communication with SR patients but also by various types of quality care provided to them, such as offering medication, supporting nutrition and hydration, assisting in personal hygiene, and observing the somatic condition. Thus, any evaluation of how these tasks are accomplished must examine the patients' own rigorously measured perceptions of both the SR itself and the overall treatment related to SR.

Among the existing questionnaires examining how SR is perceived, some focus on negative emotions such as fear, hopelessness and punishment, or about positive experiences such as a calming effect or feeling of safety. Other questionnaires directly ask about the efficacy of SR.[2–5,17] The surveys of involuntarily admitted patients' perceptions of their treatment include questions referring to the involuntary admission itself such as perceived coercion, being respected and feeling safe, and those asking about the relationship with care staff, perceived improvement and satisfaction.[18–21] Most of those surveys explain the results by item individually, but do not provide a discussion using a composite score of each item, to grasp the overall aspects of patient perceptions.

In contrast, several questionnaires addressing patient satisfaction and collaboration between the patient and care staff were designed as a measurement using the total score, but did not include items specific to SR.[22–25] Moreover, some of them involve many questions, which imposes an excessive burden on a patient just after an SR event.

Accordingly, a questionnaire that measures all of the aforementioned aspects of patient perceptions in only a few items, to reduce patient burden, does not exist.

The aim of this study was to develop a self-reporting questionnaire as a tool for measuring patient perception in order to evaluate the quality of overall treatment related to SR – a questionnaire applicable even to emotionally labile patients right after an SR event.

METHODS

Scale development

To determine the items that would constitute the new questionnaire (hereafter referred to as the 'Secluded/Restrained Patients' Perceptions of their Treatment', SR-PPT), the items used in previous surveys and existing questionnaires were examined. These included surveys on perception of SR[2–5,17] and involuntarily admitted patients' perceptions of their treatment,[18–21] questionnaires on patient satisfaction,[22,23] and the Working Alliance Inventory (WAI).[24,25] The items identified from the existing questionnaires for development of the SR-PPT were reviewed by a professional group consisting of two psychiatrists, three psychiatric nurses and one psychiatric occupational therapist. In total, 17 items were selected and categorized into the following five domains: 'working alliance for treatment' (seven items) and 'respect and autonomy' (four items), which are considered to be the domains most influenced by the coercive manner of SR; and second, 'how patients felt about their SR' (three items), and then 'satisfaction' (two items) and 'perceived improvement' (one item) as general impressions. With regard to the number of items, careful consideration was given to minimize the survey-related burden on patients who might be distressed during or immediately after SR.

The SR-PPT consists of several existing items in English and new items originally drafted by the main author (T.N.) in Japanese. Both English and Japanese versions of the SR-PPT were prepared. Permission was obtained from all authors of the existing questionnaires in order to use the exact wording of the items. The existing items in English were translated into Japanese by the same author (T.N.) and back-

translated into English by two independent native speakers. The back-translation was checked against the original English sentences by another native English-speaking psychiatric care worker. The original items in Japanese were translated into English by two independent native English speakers and then back-translated into Japanese. The back-translation was then checked by the same author (T.N.).

A 100-mm visual analogue scale (VAS) was chosen as the measurement scale, allowing responses ranging from 'strongly disagree' to 'strongly agree' (scored correspondingly from 0 to 100 mm). Respondents were requested to answer based on their perceptions at the time of filling in the questionnaire and not to recall retrospectively the feelings experienced during SR.

The study was conducted between May and August 2008.

Setting

Two emergency wards and one acute ward in two psychiatric hospitals (N Hospital and K Hospital) in Japan participated in the study. 'Emergency ward' and 'acute ward' are ward categories stipulated by the national reimbursement system in Japan. The emergency and acute wards are those with ≥40% of patients newly admitted and with ≥40% of the newly admitted patients discharged to their home within 3 months. Emergency wards must also accept a required minimum number of compulsory involuntary admissions under orders from the hospital's catchment area. Accordingly, the average registered nurse allocation for an emergency ward is 10 patients per nurse per day (vs 13 patients per nurse per day for an acute ward).

The characteristics of the participating wards (emergency ward in N hospital, emergency ward in K hospital and acute ward in K hospital) are, respectively, as follows: number of beds, 60, 26 and 44; mean hospital stay days, 56.7, 25.0 and 37.7 days (in 2007); mean seclusion days per 1000 patient-days 176, 487 and 154 (in February 2008); and mean restraint days per 1000 patient-days 24, 32 and 5 (in February 2008). All three wards were mainly responsible for patients with schizophrenia or schizophrenia-related disorders (F 20-F29 category of the ICD-10).

Participants

The inclusion criteria were: age 18–65 years, an SR episode during current hospitalization, and written informed consent from the patient and his/her family (mandatory in Japan). Patients were excluded if they were receiving i.v. infusion due to a somatic disease, if their psychiatrist in charge did not agree to cooperate with the researchers, or if their clinical condition prevented their participation as judged by their psychiatrist.

Eligible candidates were selected by checking the patient records. At the same time, baseline variables (sex, age, diagnosis, number of admissions), duration of current hospitalization, interval from last SR treatment event until the date of survey and total duration of all SR treatment events were obtained for each of the eligible candidates.

Assessment

Prior to filling out the SR-PPT, the investigator showed the patient how to fill in the VAS and the patient practiced answering the questionnaire using an example. The patient then filled in each VAS of the 17 items of the SR-PPT.

Following the SR-PPT, the patient filled in another newly developed VAS form, enquiring how much difficulty, fatigue and strain they felt when answering the SR-PPT.

To evaluate the criterion-related validity of the SR-PPT, the Japanese version of the Client Satisfaction Questionnaire-8 (CSQ-8J) was filled out on the same occasion. The CSQ-8J is a measurement tool to rate the patients' satisfaction of a care service and contains eight items, all 4-point Likert scales. The overall score ranges from 8 to 32, and higher score indicates higher satisfaction.[22] It has been widely used with patients as part of the outcome assessments for health and welfare services.

There exists evidence of a correlation between the subjective outcome evaluation (completed by the patient him/herself) and the objective outcome evaluation (symptom assessment by a rater).[13,26] To assess such a kind of correlation between additional external criteria and the SR-PPT, the following assessments were performed by the psychiatrist in charge on the same day as the SR-PPT: the Brief Psychiatric Rating Scale (BPRS; 18 items, score range 1–7),[27] the Global Assessment of Functioning (GAF)[28] and GAF improvement (change from the admission date).

Ethics

The study was approved by the Ethics Review Board of the National Center of Neurology and Psychiatry.

In accordance with the national ethics requirement to first obtain proxy consent for research participation of an involuntarily admitted patient with limited comprehension, consent from the patients' relatives was obtained. Before completing the survey, all eligible patients for whom the informed consent by proxy was obtained were given a comprehensive description of the study and informed that their participation or refusal would not affect their care. Patients were informed that the ward staff would not see their SR-PPT responses, that the completed questionnaire would be sealed in an envelope directly in front of them and that the data would be treated anonymously. Thereafter their own written consent was obtained.

Taking into consideration the fact that some of the patients were currently under treatment programs that included SR, the main author (T.N., a psychiatrist) carefully observed the patient's level of fatigue or irritability and discontinued the procedure when necessary. In addition, after completing all of the questionnaires, the ward head nurse monitored the patients for any deleterious symptoms that might have been induced by the study procedure.

Statistical analysis

For the 86 participant candidates who met the inclusion criteria, the differences in patient characteristics between those who completed the SR-PPT and those who did not were analyzed using Student's *t*-test for continuous variables of normal distribution (Shapiro–Wilk test, $P \geq 0.1\%$) and the Mann–Whitney *U*-test for variables of non-normal distribution (Shapiro–Wilk test, $P < 0.1\%$). The χ^2 test was applied for categorical variables. The reliability was estimated by identifying factors using factor analysis (main factor method) and by examining the internal consistency of the subscales using Cronbach's alpha coefficient. The concurrent validity was estimated using Pearson's correlation coefficient between the SR-PPT score and the CSQ-8J score. To estimate the correlation of SR-PPT score with the external criteria, Pearson's correlation coefficient (for GAF and BPRS) and the partial correlation coefficient (for GAF improvement) were used. The relationship between patient characteristics and patient burden induced by answering the SR-PPT was tested using Pearson's correlation coefficient for continuous variables of normal distribution, and Spearman's rank correlation coefficient for variables of non-normal distribution. For categorical variables, one-way ANOVA was applied. The significance level was set according to two-tailed test. All statistical analyses were performed using SPSS version 15.0 (SPSS, Chicago, IL, USA).

RESULTS

Of 182 patients hospitalized on the study wards on the date of the survey, 110 patients were aged 18–65 years and had experienced SR. Of these, nine patients had been discharged prior to the survey date, five patients were treated by physicians who refused to cooperate in the study and 10 patients were, according to their attending psychiatrists, unable to tolerate the study procedure. Of the remaining 86 patients, two patients did not volunteer their consent. The families of 27 more patients could not be contacted by the staff and proxy consent was thus not obtained. One patient was excluded by the main author (T.N.) due to the patient's excessive fatigue while answering the questionnaire. Finally, the SR-PPT was completed fully by a total of 56 patients.

Patient characteristics are listed in Table 1 including the mean GAF and BPRS scores. There were no

Table 1. Patient characteristics ($n = 56$) and GAF/BPRS scores

	n, mean ± SD, or median (IQR 25%–75%)	%
Sex		
Male	31	55
Age (years)	42.4 ± 13.0	
Diagnosis[†]		
F20–F29	39	69
F30–F39	11	20
F10–F19	4	7
Others	2	4
No. admissions	1.5 (1.0–4.0)	
Days between last seclusion/restraint event and investigation	10.0 (3.5–38.5)	
Days between admission and investigation	36.0 (16.0–64.0)	
Days of seclusion	12.0 (6.0–21.0)	
Days of restraint[‡]	5.0 (2.0–8.0)	
GAF at admission	27.9 ± 11.4	
GAF at investigation	49.8 ± 16.3	
BPRS at investigation	40.1 ± 15.3	

[†]International Classification of Disease Tenth revision (ICD-10); [‡]20 patients experienced restraint.
BPRS, Brief Psychiatric Rating scale (18 items, score range 1–7); GAF, Global Assessment of Functioning.

significant differences in the patient characteristics between the 56 participants and the 30 excluded patients.

Factor analysis

Principal factor analysis on the 17 items selected as candidates was performed, because none of the 17 items exhibited ceiling or floor effects. The eigenvalue shifts were 9.80, 1.48, 1.1 and 0.85, assuming that the two-factor structure was valid. In addition, one item having low commonality of 0.224 following factor extraction was removed. At this point, a two-factor hypothesis emerged and factor analysis was performed using the principal factor method and varimax rotation. Next, the five items with a loading of $\geq$0.35 on both the primary and secondary factors were removed. The factor analysis was then repeated using the principal factor method and varimax rotation on the remaining 11 items. Table 2 lists the final factor pattern following varimax rotation. Incidentally, the ratio explaining the total variance of the 11 items for the two factors prior to rotation was 64.5%. In the nine primary factor items, those items that involved communication with staff toward mutual understanding of the treatment process and goals had a high loading and were therefore named 'Cooperation with Staff'. In the two secondary factors, those items involving perceptions of SR had a high loading and were thus named 'Perceptions of SR'.

Internal consistency of the SR-PPT

The subscale coefficient alpha was also calculated in order to evaluate internal consistency. Adequate alpha coefficients were obtained for Cooperation with Staff (0.928) and Perceptions of SR (0.887). The value for the 11 items of the SR-PPT was 0.916.

SR-PPT scores

The mean ± SD total score for all the final 11 items (ranging from 0 to 1100) was 658.7 ± 245.4, and the mean subscale scores for Cooperation with Staff (max. 900) and for Perceptions of SR (max. 200) were 559.3 ± 208.9 and 99.4 ± 65.9, respectively. Correlations between each subscale score and the total score were observed as shown (Table 3). No significant differences nor correlations between ST-PPT total scores and the patient characteristics (sex, age, diagnosis, number of admissions, days between last SR event or admission and investigation, and days of SR) existed.

Criterion-related validity

The mean ± SD CSQ-8J score was 21.7 ± 5.6. Significant correlations were observed between CSQ-8J

Table 2. Rotated factor matrix for 11 items of the SR-PPT

	Factor loading	
	1	2
Factor 1: Cooperation with staff		
Do you and the staff agree about the things you will need to do in treatment to help improve your situation?	0.838	0.204
Are you and the staff working towards mutually agreed upon goals?	0.832	0.323
Do you feel that the staff members understand your concerns?	0.825	0.251
Have you been respected on the ward as a person?	0.810	0.333
Is your opinion taken into account with regards to your treatment?	0.746	0.184
Are you being given enough time during your treatment or care?	0.737	0.216
Do you collaborate with the staff on setting goals for your treatment?	0.685	0.066
Can you voice your opinion?	0.667	0.130
Do you feel that staff members have ignored you in any way?	0.557	0.176
Factor 2: Perception of seclusion/restraint		
Was being restrained and/or secluded beneficial in treating your difficulties?	0.202	0.868
Was it necessary for you to be restrained and/or secluded?	0.228	0.860
Factor contribution	5.96	1.13
Contribution variance rate	54.2%	10.3%

SR-PPT, Secluded/Restrained Patients' Perception of their Treatment.